Spread spectrum techniques in BCI:

A review of auditory and visual BCI-systems using continuous and binary noise tagged stimuli

Author: Abraham Jannis van Duijn[1]

Thesis submitted to the Graduate School of Life Sciences of the Utrecht University, Utrecht in partial fulfilment of the requirements for the degree of Master of Science 2012

Supervisors: prof. dr. ir. P. Desain[2] **and prof. dr. N.F. Ramsey**[3]

[1] *Graduate School of Life Sciences*
Neuroscience and Cognition Master Program
Utrecht University, Utrecht, The Netherlands

[2] *Faculty of Social Sciences*
Section Artificial Intelligence / Cognitive Science
Radboud University, Nijmegen, The Netherlands

[3] *Department of Neurology and Neurosurgery*
Section Brain Function and Plasticity
Rudolf Magnus Institute, Utrecht, The Netherlands

May 1st. 2012

ABSTRACT

Title of document:	Spread spectrum techniques in BCI: A review of auditory and visual BCI-systems using continuous and binary noise tagged stimuli
Author:	Abraham Jannis van Duijn, BSc
Supervised by:	Prof. dr. ir. Peter Desain, Artificial Intelligence / Cognitive Science, Radboud University, Nijmegen Prof. dr. Nick F. Ramsey, Department of Neurology and Neurosurgery, Rudolf Magnus Institute, Utrecht

Brain computer interfaces (BCIs) are an essential tool for locked-in patients, providing a link with the outside world. However, the type of stimuli used in most brain computer interface system may have a detrimental influence on the information transfer rates (ITR) achieved. Steady state evoked potentials (SSEP) have been well studied and applied in EEG-based BCI-systems, reaching high ITRs, but the number of SSEP-stimuli that can be applied simultaneously is limited. These responses also suffer from noise due to spontaneous oscillations that occur in the brain.

In spread spectrum techniques, signals are distributed over a broader bandwidth in a pseudorandom fashion, making them much more robust against interference from noise or cross-stimulus interactions. Broadband noise signals have been successfully used in other neurological disciplines, but have remained a relatively neglected class of stimuli in BCI-systems.

Spread spectrum elicited evoked potentials offer a valuable extension of the palette of AEPs and VEPs available for BCI-systems, as their favourable auto- and cross-correlation characteristics provide good anti-interference properties, which make them especially beneficial in systems using multiple simultaneously presented stimuli, like speller-setups.

This thesis gives an introduction into spread spectrum techniques and the pseudorandom noise sequences used herein. The limited number of auditory and visual BCI-systems using continuous and binary noise tagged stimuli are reviewed and compared. Some of these systems reached information transfer rates of >100 bits/min. showing the potential of this approach.

ACKNOWLEDGEMENTS

I would like to express my gratitude to the following individuals/groups:

1. Professor Peter Desain, for offering me the opportunity to write this thesis and the supervision given during the process. It was a pleasant collaboration.

2. Professor Nick Ramsey, for examining the final thesis.

3. Andrei Belitski and Gijs van Duijn, for proofreading my concept versions and offering valuable suggestions.

4. All the people at the Cognitive Artificial Intelligence department of the Radboud University Nijmegen and the CAI BCI group at the Donders Centre for Cognition for offering a welcoming work environment, as well as pleasant lunch and coffee breaks.

5. My family and roommates, for their mental and social support and keeping up with me in the more stressful periods.

CHAPTER 1 – INTRODUCTION

Introduction into Brain Computer Interfaces - Possible uses

Envision yourself controlling a robot with thoughts, by merely thinking what you want it to do. Whereas this used to be the domain of science-fiction writers, advances in brain imaging technology and cognitive neuroscience are bringing the future into the present. Brain-computer interfaces (BCIs) which extract mental activity to directly control a computer or prosthetic device are becoming more and more sophisticated. Communication with and control of a computer without using brain-motor periphery communication channels is especially useful in the rehabilitation of patients with severe motor impairments (N. Birbaumer et al., 1999; N. Birbaumer & Cohen, 2007; Hochberg et al., 2006; Kübler et al., 2005; Nicolelis, 2003), but holds a large array of possible applications, including biofeedback therapy for neurological disorders (Christopher deCharms, 2008; Hamadicharef et al., 2009; Leins et al., 2007), control of assistance systems (Scherer et al., 2007; Velliste, Perel, Spalding, Whitford, & Schwartz, 2008), mental state monitoring (Zander & Jatzev, 2009), gaming (A. Nijholt, Tan, Allison, Milan, & Graimann, 2008; A. Nijholt, Bos, & Reuderink, 2009; Plass-Oude Bos et al., 2010; Reuderink, 2008), industrial robot control (Biao Zhang, Jianjun Wang, & Fuhlbrigge, 2010), and building adaptive user interfaces (A. Nijholt & Tan, 2008). Although the motivation for development of this technique predominantly was focussed on improving the lives of motor impaired patients, this list also shows the possibilities of this technique in healthy individuals. For a recent overview of medical uses of BCI see (Pasqualotto, Federici, & Belardinelli, 2012; Rothschild, 2010), non-medical uses of BCI see (Blankertz et al., 2010), and state-of-the-art BCI's (Nicolas-Alonso & Gomez-Gil, 2012). For ethical considerations concerning BCIs, see (Haselager, Vlek, Hill, & Nijboer, 2009; Nijboer, Matuz, Kübler, & Birbaumer, 2006; Nijboer, Clausen, Allison, & Haselager, 2011a; Nijboer, Clausen, Allison, & Haselager, 2011b; Tamburrini, 2009).

Introduction into Brain Computer Interfaces - A general BCI model

A functional model of a generic BCI system is shown in figure 1.1 (Gerven et al., 2009). Traces of brain activity of a user performing a cognitive task are measured (signal extraction) and pre-processed (for signal enhancement), relevant features are then extracted and used to classify the predicted intention of the user. This prediction is translated into control signals for an external device. The user's observance of the changed behaviour of the device completes the cycle, allowing judgement about the correctness of the prediction and adaptation of the mental activity. The prediction can also be fed back to the user in a more explicit way, allowing for a more robust evaluation of the classification. Iterating through the cycle allows both user adaptation and machine-learning. This mutual adaptation can in principle increase the overall performance of the system but can also be hard to analyse and control and could become the cause of instability.

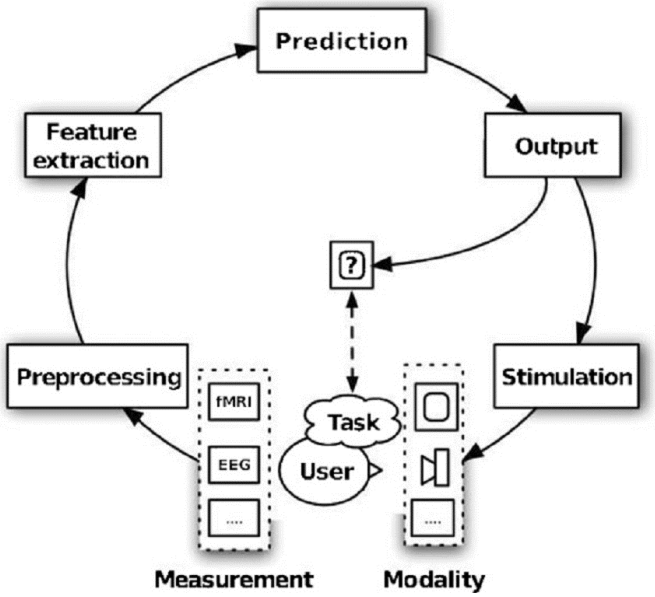

Figure 1.1: The different steps in the brain computer interface cycle. The user receives stimuli while performing a cognitive task. Sensors measure traces of the brain signals, which are then pre-processed (signal enhancement), useful features are extracted and a classifier uses these features to predict the user's intention. This outcome is then used to control an external device. The circle is closed when the output is feed back to the user, either explicitly or indirectly by the user perceiving the device's behaviour, allowing for judgement of the decision and adaptation by the user.
[From: (Gerven et al., 2009) – figure 1]

The performance of a BCI system can be quantified in a number of ways. A recent survey showed that high accuracy and speed of operation are regarded as the most important performance criteria under BCI-users (Huggins, Wren, & Gruis, 2011). The accuracy is described as the percentage of correctly classified results, or its inverse the error rate. The speed of the system is usually described in the number of bits (basic units of information) that can be transmitted between the user and the system in a certain time, the information transfer rate (ITR) (Kronegg, Voloshynovskiy, & Pun, 2005). The signal-to-noise ratio (SNR) is an important measure of the quality of the measured signals, and is often expressed in decibels (dB).

Signal extraction can be performed using a multitude of brain imaging techniques. These can be invasive techniques using implanted electrode arrays recordings (local field potential. microelectrode (ME) and ME-array recordings, and electrocorticography (ECoG)) or non-invasive, such as electroencephalography (EEG), magnetoencephalography (MEG), functional magnetic resonance imaging (fMRI), and near-infrared spectroscopy (NIRS) (Wolpaw et al., 2006). EEG and MEG, reflecting averaged activity of (respectively extracellular and intracellular) dendritic currents of large population of neurons, provide a high temporal but poor spatial resolution. MEG has a somewhat higher spatial resolution than EEG, but needs strong magnetic shielding, making it less practical. fMRI has a high spatial resolution, but since it uses haemodynamic

changes as a metabolic proxy for brain activity, introducing a physiological delay from 3 to 6 seconds (Weiskopf et al., 2004), it suffers from poor temporal resolution. NIRS uses the same intermediary as fMRI and is limited to cortical tissue. The invasive methods offer much better performance both spatially and temporally, but pose significant health hazards, limiting the use of these methods to animal studies and severely impaired patients. Therefore EEG is the preferred method to measure the brain activity in most of the current BCI studies.

EEG-based Brain Computer Interfaces - Major paradigms

The pre-processing steps that are necessary depend on the stimulus modality, imaging technique and feature type used. Visual and auditory stimuli are most often used, although some groups also use somatosensory stimuli (Breitwieser, Pokorny, Neuper, & Muller-Putz, 2011; Muller-Putz, Scherer, Neuper, & Pfurtscheller, 2006; Ortner, Allison, Korisek, Gaggl, & Pfurtscheller, 2011), or a combination of these modalities (Gürkök & Nijholt, 2011; Maye, Zhang, Wang, Gao, & Engel, 2011; A. Nijholt, Allison, & Jacob, 2011; Zhang et al., 2007). In EEG-based BCIs there are a few major paradigms or types of tasks used: Slow cortical potentials (SCP), transient tags (P300), steady state evoked potentials (SSEP), and motor imagery (ERD/ERS).

SCPs are slow voltage shifts in the EEG lasting several seconds (N. Birbaumer, Elbert, Canavan, & Rockstroh, 1990), which (after training) can be voluntarily changed and used to move a cursor on a computer screen (Hinterberger et al., 2004). SCP has acceptable accuracy rates (70-80%), but is hindered by extensive training requirements and a relatively low ITR of 5-12 bits per minute (Nicolas-Alonso & Gomez-Gil, 2012).

P300 uses an infrequent and unexpected target stimulus shown among several frequent non-target stimuli to evoke an event-related potential, visible as a positive peak in the EEG signal about 300ms after attending the oddball stimulus. A typical utilization of a visually evoked P300 is a speller application using a letter matrix with randomly flashing rows and columns (Farwell & Donchin, 1988). P300-based BCIs require no user-training sessions, although performance can decrease after prolonged use as the subjects habituates to the infrequent stimuli (Ravden & Polich, 1999). The ITR is limited to 20-25 bits/min. as the low signal-to-noise ratio (SNR) forces the classifier to average over multiple trials (Nicolas-Alonso & Gomez-Gil, 2012).

Motor imagery uses mental tasks to change the amplitude of oscillatory activity in certain frequency bands in the EEG signal, specifically in the mu- (7–13 Hz) and beta-rhythms (13–30 Hz). These event-related desynchronization (ERD) and synchronization (ERS) have been measured over the sensorimotor cortex during motor imagery tasks (Pfurtscheller & Lopes da Silva, 1999; Toro et al., 1994), but can also be found during other mental tasks (Gerven et al., 2009). The ITR is between 3-35 bits/minute, but as with SCP-based BCIs extensive training is needed (Nicolas-Alonso & Gomez-Gil, 2012).

Steady state evoked potentials (SSEP) use stimuli with a repetitive character that give a strong and traceable evoked response. It is postulated that the periodic stimulation induces frequency- and phase-locking responses in neural circuits, provoking the SSEP (Regan, 1977). Selective attention to a stimulus influences the power and phase of the signal, allowing the BCI system to distinguish between multiple stimuli (Middendorf, McMillan, Calhoun, & Jones, 2000). SSEPs have been used primarily in the visual system (SSVEPs, see (Vialatte, Maurice, Dauwels, & Cichocki, 2010) for a review), but also in the auditory system; auditory steady-state response (ASSR, see (Plourde, 2006) for review), and to a much lesser extent in the tactile system; the steady state somatosensory evoked response (SSSEP) (Muller-Putz et al., 2006). (SS)VEP-based BCI systems managed to arouse interest of a number of research groups, as it offers a high ITR (60-100 bits/min.) with a high number of possible (simultaneous) stimuli, without the need of extensive training (Nicolas-Alonso & Gomez-Gil, 2012; Volosyak, 2011).

Next to these, there are methods to track covert selective (visual) attention independent of stimulation in e.g. lateralized alpha (Bahramisharif, Van Gerven, Heskes, & Jensen, 2010). They don't require use training, but the steady fixation is often difficult to achieve in practical BCI's. In this thesis we will restrict ourselves to BCI's based on stimulus processing.

EEG-based Brain Computer Interfaces - VEP modulations

In (visual) evoked potential based BCI-systems the stimulus sequence design has a big effect on the performance of the system. Three categories of VEP modulations can be distinguished: time modulated VEP (t-VEP), frequency modulated VEP (f-VEP), and pseudorandom code modulated VEP (c-VEP). In t-VEP the flash sequences of multiple targets differ in time, being either strictly non-overlapping, or having a stochastic distribution. Targeting is achieved by fixating on a target, as foveal flash VEPs are larger than peripheral flash VEPs. As in P300 t-VEP BCI requires averaging over multiple trials, limiting the ITR to under 30 bits/min.(Bin, Gao, Wang, Hong, & Gao, 2009). f-VEP is a form of SSEP, as each target is flashed at a distinctive frequency, causing a periodic sequence of evoked responses with the same fundamental frequency as the flickering target, as well as its harmonics. It offers a simple setup, demanding no user training and provides an ITR of 30-60 bits/min.(Bin et al., 2009). In c-VEP the duration of the flashes of each target is determined in a pseudorandom manner, typically using m-sequences. The cross- and auto-correlation properties of these m-sequences allow signal modulations that optimize the ITR, reaching speeds up to 100bits/min. (Bin et al., 2009; Bin et al., 2011; E. E. Sutter, 1992).

Introduction of spread spectrum techniques

The pseudorandom methods used in c-VEP found their origin in the spread spectrum transmission technique developed in the 1950's. Spread spectrum is a technique of transmission of a signal in which the signal occupies a broader bandwidth than minimally required to send the information. The band spread is achieved by a (pseudorandom) code which is independent of the data, and a synchronized reception with the code at the receivers end is used for despreading and subsequent data recovery (Pickholtz, Schilling, & Milstein, 1982). There are a number of benefits in spreading the signal, like

robustness against (un)intentional interference and noise, low spectral density, reduction of multipath effects (self-interference by overlap of time-delayed signals), and multi-user access.

Spread spectrum for mental tasks based BCI
The benefits of tagging the stimuli with a spread spectrum signal may translate into robustness for BCI. In these systems multiple stimuli are presented in parallel and their signatures may all be found in the brain response. For visual BCI's eye gaze may be used a means of selecting one of them as target. But also selective attention as a higher level cognitive process may be active. For other modalities where the perceptual sense can be less easily directed at a physical level, selective attention is the main process that allows BCI's to work. The spread spectrum nature of the tags make them optimally distinguishable in the measured brain signals - even in the context of a not completely known perceptual system that processes the stimuli in unknown timeframes, induces crosstalk, and may cause large disturbing signals, like spontaneous brain oscillations.

Goals of this thesis
The benefits of spread spectrum, especially the noise robustness and multi-user access possibilities, make that the spread spectrum transmission technique might also prove useful for stimulus delivery, trailing and tracing the response in BCI and other neurologic research. This thesis aims to elaborate this statement by giving a theoretical background into the components of this technique, elucidate the advantages and inconveniences, and giving an overview of (BCI) studies performed using (components of) this technique. Concrete questions that will be addressed are:

> Which BCI-related studies have been performed using spread spectrum signal transmission techniques and/or pseudo randomly generated sequences?
>
> Are these studies comparable, and if they are, how do the methods used and results obtained match?
>
> Which pseudo randomly generated sequences provide the best properties for use in auditory and visual BCI-systems and what are the most optimal parameter-ranges?
>
> When offering multiple stimuli simultaneously, how can targeting be accomplished?

Overview of this thesis
Chapter 2 gives an introduction in Spread Spectrum techniques, presenting techniques to spread the signal over a broader bandwidth and examining the sequences (codes) used in these variants. During the explanation the accentuation might be on the uses of and advantages of this technique in telecommunication, but at the end of the chapter the connection with neuroscience will be established again.

Chapter 3 and 4 provide an overview and comparison of the auditory and visual BCI related studies that have been performed using spread spectrum signal transmission techniques and/or pseudo randomly generated sequences. Important points of evaluation will be the information transfer rate, signal-to-noise ratio, performance, sensitivity and the number of simultaneous stimuli. At the end of each chapter recommendations will be distilled out of the discussed studies.

Chapter 5 will conclude the thesis with a discussion about the potential and challenges of the use of this technique in brain research and will also summarize the recommendations for codes and parameters, as well as suggest some future research.

CHAPTER 2 – SPREAD SPECTRUM TECHNIQUES

History of spread spectrum transmission techniques

The first referral to a spread spectrum signal modulation for communication was dividing the signal over multiple frequency bands, switching ('hopping') from one band to another as time passed. This concept of frequency hopping was proposed by Nikola Tesla in 1900 as a secure method for radio-control of a submersible boat (Hammond & Purington, 1957). During the first and second world war it was used on a limited scale in communication. Spread spectrum techniques were further developed in the 1950's by both the U.S. and U.S.S.R. military for communications and guidance systems among others, mainly due to the strong anti-jamming and anti-interference capacities, as distributing a relatively low dimensional signal in an high dimensional environment forces the jammer to distribute his power either over all frequencies, blocking each only a little, or block a small range of frequencies completely, while leaving the others untouched. Also, by spreading the signal into a noise-like carrier wave, it makes signal detection and interception itself very difficult without the code sequence, thereby offering an extra layer of privacy (Cook & Marsh, 1983; Pickholtz et al., 1982).

It offers the possibility of multi-user random access: multiple simultaneous transmissions between different users can take place in the same spectral band, by combining spread spectrum transmission with special code-sequences, so called Code Division Multiple Access (CDMA). This makes the technique very useful for (mobile) communication, as multiple users can use the same frequency bands at the same time without interfering each other. The first civilian forms of spread spectrum were developed in de 1950's, but commercial use didn't take place until the 1980's, when low cost, high density digital integrated circuits became available, making miniaturization possible. Nowadays it is used on a massive scale in (amateur) radio, wireless communication (UMTS, Wi-Fi, and Bluetooth), localization (GPS) and satellite communication.

Spreading the signal

The spectrum can be spread in a number of ways. In so called "direct-sequence modulation" a pseudo randomly generated sequence (pseudo random noise code or PN code) is 'multiplied' (or 'ex-or-ed') by the carrier containing the data. The PN-code consists of elements ("chips") valued -1 and 1 (polar), or 0 and 1 (non-polar). The frequency of the PN sequence (the "chipping rate", f_C) is much higher than the frequency of the data signal (f), meaning that one symbol (bit) is represented by multiple chips. The ratio between the chip time (T_C) and the pulse time of the data signal ($T=1/f$, also known as the symbol rate) is known as the spreading factor (SF) or processing gain (figure 2.1) (Meel, 1999; Pickholtz et al., 1982).

In "frequency hopping" the signal is spread over a wide frequency range, by dividing the total bandwidth in N sub-bands, and the transmitter changing the carrier frequency (the signal) from one sub-band to another, 'hopping' in a pseudorandom fashion (figure 2.2). A division can be made whether the first one or more bits are encoded in a single hop, so called "slow frequency hopping" (SFH), and dividing one bit over multiple hops, "fast frequency hopping" (FFH) (Cook & Marsh, 1983; Meel, 1999).

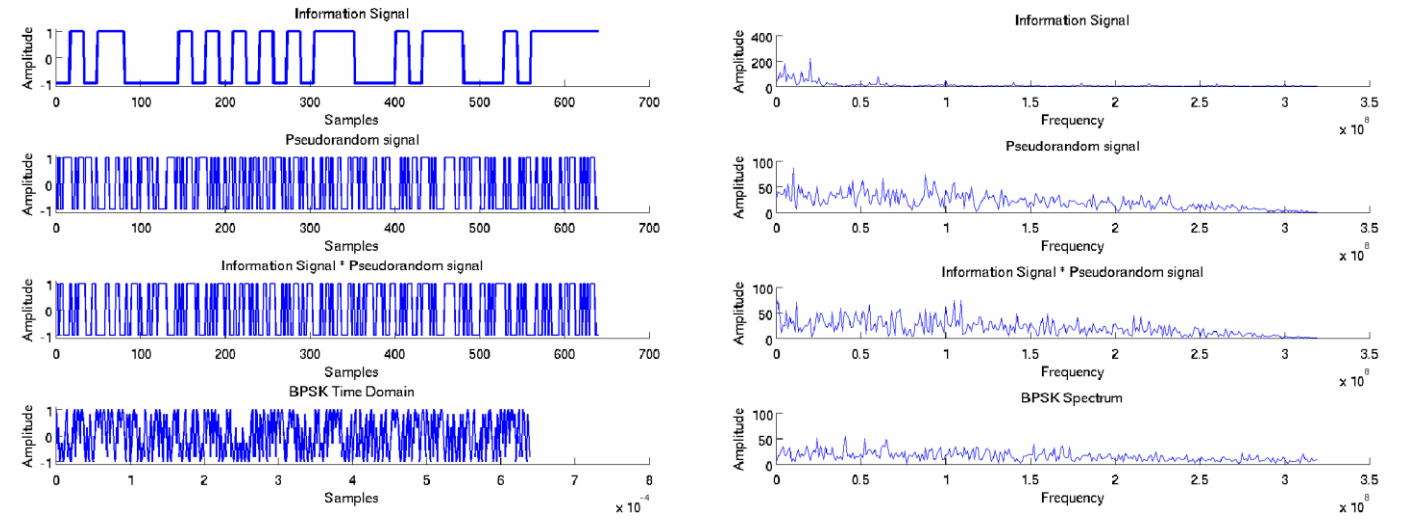

Figure 2.1: Direct-sequence spread spectrum modulation. On the left the signal and on the right the spectrum of the signal is shown. The data signal (top) is multiplied with a pseudo random generated sequence of much higher frequency (second from top), resulting in a modulated sequence (third from top). This sequence is spread over the spectrum by multiplying it with a carrier wave (i.e. *cos(ω*t)*), resulting in a spread signal (bottom). [From: (Longstreet, 2008) - figure 2+3]

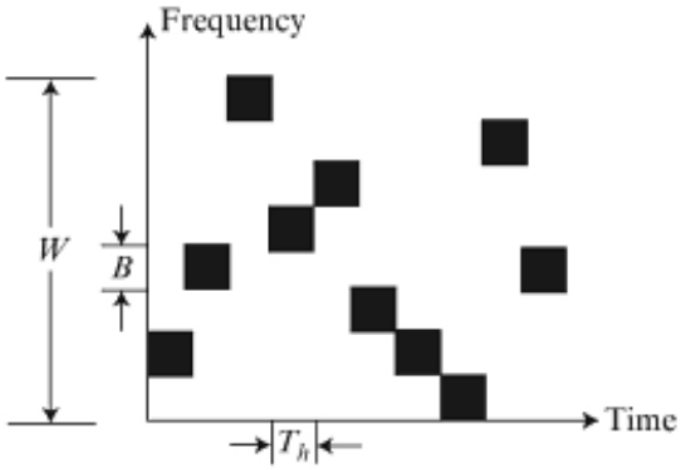

Figure 2.2: Frequency hopping spread spectrum modulation. The total frequency band (W) is divided in a number of sub-bands with bandwidth B. The transmitter uses a certain sub-band for a limited time (T_h), and then switches to another sub-band. To minimize chance of detection and interference this hopping is performed in a pseudorandom order.
[From: (Torrieri, 2011), page 150 - figure 2.1]

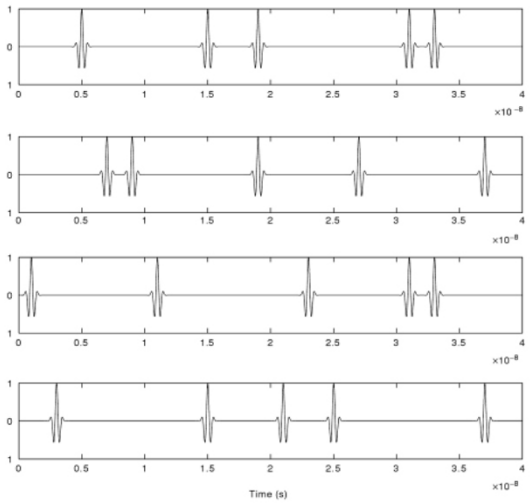

Figure 2.3: Time-hopping spread spectrum modulation. The frequency channel is shared by multiple users and is divided in multiple time-slots, each user sends only during the timeslots assigned. Transmission times are determined by pseudorandom sequences.
[From: (Buehrer, 2006), page 44 - figure 2.15]

In "time hopping" the timing of bursts of the signal is initiated at pseudorandom times. As the frequency channel gets divided in multiple time slots, this allows several users to use the same frequency bandwidth by transmitting bursts of data in their own timeslot (figure 2.3). Hybrid combinations of these spreading techniques are frequently used in telecommunications, as each has its own advantages and disadvantages (Meel, 1999).

Benefits of spread spectrum – interference properties

In sending a signal is thus spread into a broader band. When this spread signal is transmitted it picks up interference, whether intentional (jamming) or unintentional (noise, signals from other users). In the receiver the spread signal is decoded. In this de-spreading process most of the noise picked up during the transmission is lost again. Figure 1 shows an example for narrowband interference. When the receiver despreads the signal, it correlates the received signal with the PN code used to spread the signal. This demodulation destroys the alternation introduces by the PN code, decreasing the bandwidth of the signal and increasing the power spectral density. However, when the received signal does not correlate with the PN code, the alternation is not destroyed properly and the interference is spread by the PN code over the whole frequency range, leaving only a fraction of the original noise power in the unspread bandwidth. So only the useful (information containing) signal get multiplied twice by the PN code, while the noise is only multiplied once. This enhanced signal-to-noise ratio is called processing gain and is defined as the ratio of the spread to the unspread bandwidth.

Figure 2.4 shows an example for wideband noise. Here again does the selective despreading multiply the correlated DS-signal, while decreasing the power density of the added (uncorrelated) noise. Note that this processing gain does not reduce the effects of wideband thermal noise (Gaussian noise), which has infinite power and constant energy in every direction, as the larger bandwidth of the spread signal increases the received noise power (figure 3). However, in most cases the interference is caused by a jammer with a fixed finite power.

Binary codes

Popular code sequences used in spread-spectrum transmission

The most frequently used sequences used in spread-spectrum CDMA can be divided in two classes, orthogonal (Walsh-Hadamard) and non-orthogonal (pseudo random binary sequences). Also included in this overview are some error-correcting codes which were developed more recently and have been incorporated in newer CDMA standards. First some important characteristics of the code sequences used in CDMA are introduced (Meel, 1999):

Cross correlation

The overlap between different sequences is given by their cross-correlation. For good performance of a CDMA system it is important that there is good separation between the signals of different users (low cross correlation). The receiver matches the received signal with the locally generated code of the desired user (the sender), which should give a high correlation, to retrieve the information data. However, signals meant for other receivers should correlate as little as possible, or else it will be hard to extract the appropriate signal. Lower cross correlation values allow more users in the system. When cross correlation between aligned codes is zero, the codes are considered orthogonal. While for noise codes the separation is usually expressed as correlation, for error-correcting codes usually the number of bits that differ between codes is considered and maximized, the Hamming distance.

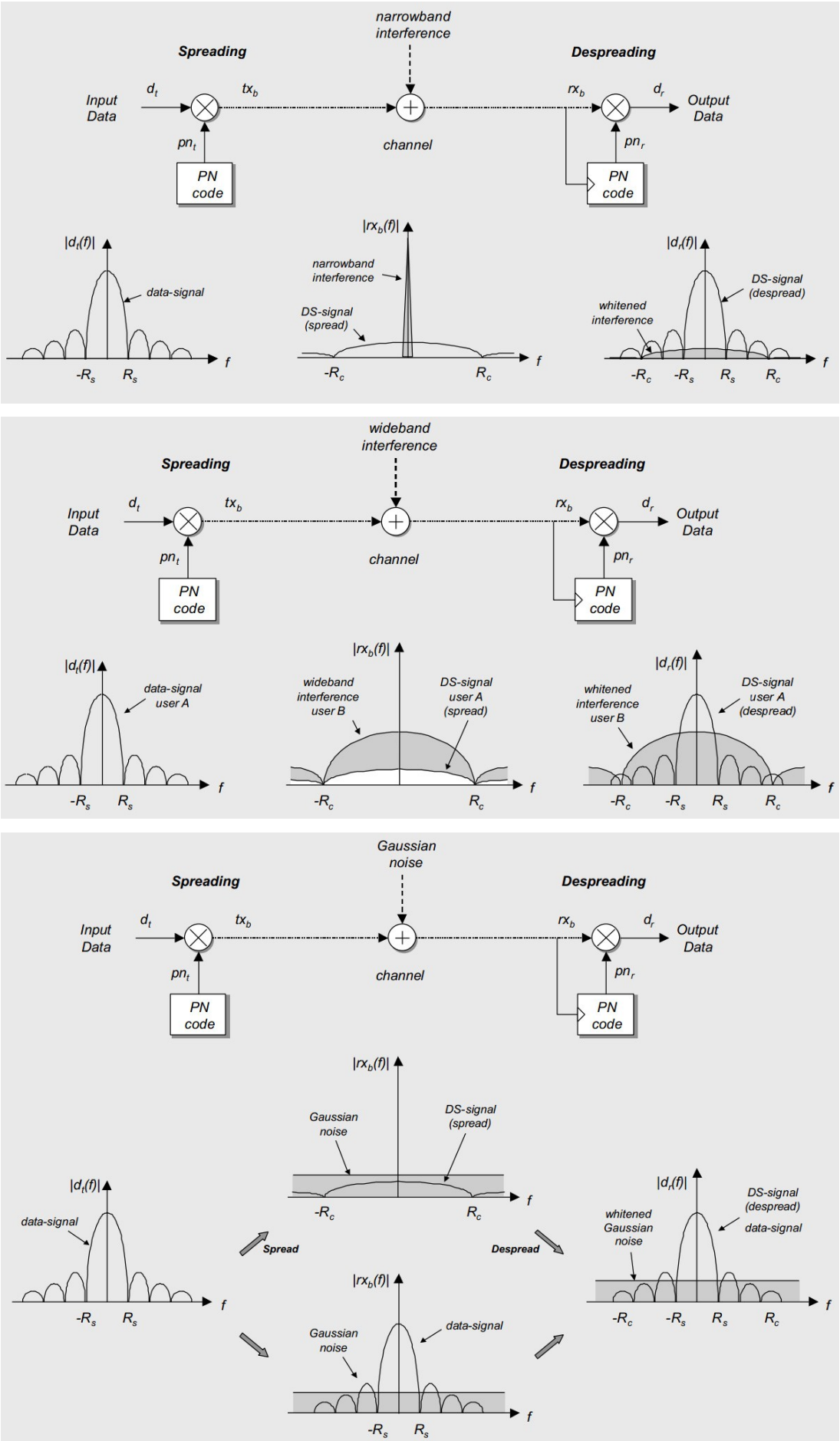

Figure 2.4: Direct-sequence spread spectrum modulation – Interference properties.
A) Narrowband interference; B) Wideband interference; C) Gaussian noise
[From: (Meel, 1999) - figures 4.1, 4.2 and 4.3]

Autocorrelation

Autocorrelation is the cross-correlation of a signal with a time-shifted version of itself. There will always be a peak of correlation at time lag zero, but when autocorrelation is not zero, there will also be peaks for other time-lagged pieces of the signal. When autocorrelation is high for other time lags than zero and there is no external synchronization between sender and receiver, it will be difficult for the receiver to detect where the starting point of the signal is, which is necessary for phase locking.

Balance

When the difference between the number of zeros and ones is either 0 or only 1, codes are called "balanced". It is a property found in some of the pseudo random binary sequences, as it is an indicator of true randomness: when a binary sequence shows true statistical randomness, the chance of occurrence of either a zero of one is equal, so the frequency of both zeros and ones should be distributed equiprobably [MG Kendall & BB Smith, 1938]. However, generating digits using a globally random process does not always result in local randomness, so a subset of a pseudorandom set of sequences is not balanced per se.

Balance has an important role in error correcting codes, as it allows detection of unidirectional errors in encoded messages. Also, balanced codes allow for parallel decoding, making them computationally much more efficient (Al-Bassam & Bose, 1990; Knuth, 1986).

When unbalanced modulation codes or carrier codes are used, spikes will show in the spectrum, causing interference with other signals as well as easing detection, thereby diminishing privacy advantages (Meel, 1999).

Pseudo randomly generated sequences

Pseudo randomly generated sequence or pseudo randomly binary sequence (PRBS) are binary sequences of *N* bits with *m* ones and *N-m* zeros, with a narrow autocorrelation peak. Pseudo-random codes are random in the sense that the value of a certain element is independent of the values of any of the other elements. For a listener without prior knowledge of the code it will appear random, as it has the same statistical properties as sampled white noise. Pseudo noise code sequences act as a noise-like carrier for spreading the signal, but are deterministic and periodic.

They can be created using a shift-register with feedback taps, commonly a shift register of a number (m) of stages is used whose input it is driven by an exclusive-or (sum modulo 2) function of some of the bits of the overall shift register value (figure 2.5) (Golomb, Welch, Goldstein, & Hales, 1967). As this is a linear function of the previous state, these are called linear feedback shift registers (LFSR). The initial value ('seed') and deterministic operation of the register make that they can be calculated locally by both sender and receiver as long as the seed and feedback function are known. As the register has a finite number of possible states, eventually (after *N* elements) it repeats itself. As the state in the register defines the next state, and there are 2^m possible states, N cannot be larger than 2^m.

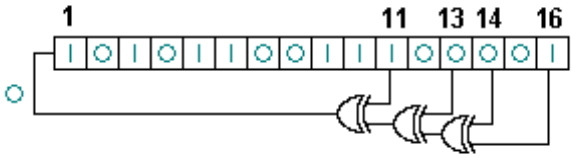

Figure 2.5: A 16-bit Fibonacci linear feedback shift register. The bit-positions that affect the next state are called taps, here [16, 14, 13, and 12]. The rightmost bit s is called the output bit and it is XOR'd with the taps and the resulting bit (a zero in this example) is fed back into the leftmost bit. The formed sequence is used as new input to calculate the next state. [From: (Cuddlyable3 at en.wikipedia, 2008)]

- *Maximum Length sequences*

A LFSR of a given size *m* (number of registers) is capable of generating every possible state during the period $N=2^m-1$, but only if proper feedback taps are chosen. An all zero input will always remain all zero, hence the minus 1in the equation. These sequences are called maximal length sequence, maximal sequence or m-sequences, have a number of special properties (Golomb et al., 1967):

M-sequences are balanced, producing $2^{(m-1)}$ ones and $2^{(m-1)}$-1 zeros.

The autocorrelation function is a very close approximation to a train of Kronecker's delta function, meaning that it has a (nearly) two-valued autocorrelation function, with a peak at time-lag zero and (near) zero elsewhere.

M-sequences have a run-length property, meaning that of all the sub sequences ("runs") of each type (runs consisting of '1' and runs consisting of '0'), half of the runs are of length 1, a quarter are of length 2, an eight are of length 3 etc.

M-sequences have a good distribution of the power over the whole frequency range, a sync2-envelope spectrum.

The modulo-2 sum of an m-sequence and a time-delayed version of that sequence yield another time-delayed version of that sequence, this is called a shift-and-add property.

- *Gold codes*

Combining two m-sequences of the same length using modulo-2 adding (XOR) yields a Gold-code, and delaying the sequences with respect to each other gives other gold-codes (Gold, 1967), as depicted in figure 2.6. Using one set of m-sequences, this gives a total number of $2^{[m+2)/2]}+1$ available Gold sequences (the two original m-sequences and combinations of $2^{[m+2)/2]}$-1 shifted sequences). Some m-sequences can form a "preferred pair" for which the cross-correlation has only 3 values: -1, $-2^{[nm+2)/2]}$-1, and $2^{[m+2)/2]}$-1. When these preferred pair m-sequences are used to create the

Gold codes an important subset of the Gold codes, the so called “Preferred Pair Gold Codes”, is obtained. These give a large set of codes with good autocorrelation properties and three-valued cross-correlation (Gold, 1967). About half of the produced Gold codes are balanced (Holmes, 2007).

Although the autocorrelation properties are worse than those of m-sequences, having a three valued auto-correlation spectrum as compared to the two valued autocorrelation spectrum of m-sequences (Mitra, 2007), Gold codes offer some strong advantages. A set of Gold codes (created from one preferred pair of m-sequences) contains a large number of equal length sequences with controlled cross-correlation properties (Dinan & Jabbari, 1998).

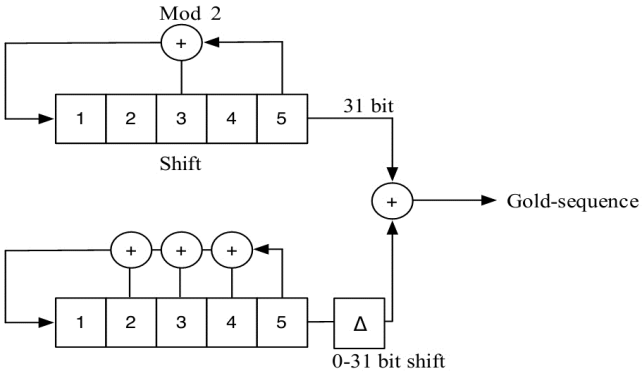

Figure 2.6: Block diagram of generation of a Gold-sequence. Two ‘preferred pair’ maximum-length sequences are modulo-2 added to form a Gold-sequence. By delaying the codes with respect to each other a large set of equal length codes can be obtained. [From: (Langton, 2002), page 8]

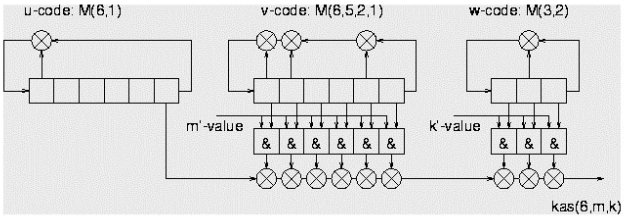

Figure 2.7: Block diagram of generation of a Kasami-sequence. Two m-sequences are combined with a decimated version of one of those sequences, resulting in a large set of Kasami-codes. [From: (Wu, 2012)]

- ***Kasami codes***

When a set of Gold code is combined (modulo-2 adding) with a decimated version of one of the 2 m-sequences that formed the Gold codes, a set of Kasami codes is obtained (figure 2.7) (Kasami, 1966). In this large set of Kasami-codes a number of special subsets can be distinguished:

- The two original m-sequences
- The Gold codes produced with these m-sequences
- The small set of Kasami-codes that can be obtained by combining a m-sequence with a decimated version of itself, so excluding the other m-sequence

The number of sequences that can be produced is $2^{(m/2)}(2^m+1)$. Two Kasami-codes from a set have a maximum cross-correlation value of $2^{(m/2)}+1$. Although this cross correlation bound is smaller than those of Gold-codes of equal length, the capacity performance of Gold codes support a user capacity twice that of Kasami codes, as performances depend on the whole spectrum of their cross-correlation function rather than their peak values (Turkmani & Goni, 1993).

- ***Barker codes***

Barker codes are finite-length pulse signals with low autocorrelation properties, as the off-peak autocorrelation coefficients are as small as possible and the maximum autocorrelation sequence has lob sides no greater than 2 (Barker, 1953). These sequences satisfy the run-length and balance properties, like m-sequences (Mitra, 2007). Unlike other PRBS’s which are periodic, Barker codes are integrable (Bar-David & Krishnamoorthy, 1996). Only a small set of 9 Barker codes is known (table 2.1), and it is presumed that no other perfect binary phase codes exist (D Terr, 2012).

Error-correcting codes

Error-correction codes are mandatory in frequency hopping systems in order to handle the high rates of error induced by partial band jamming. In other spread spectrum systems they also found some applications.

- ***Walsh Hadamard sequences***

The Walsh–Hadamard code is a linear code over a binary alphabet that maps a message of length n to a code of length 2^n. The W-H code is a locally decodable code (error correcting code), encoding the message in a redundant way, allowing the receiver to decode a single bit of a message with high probability by only looking at a small number of bits of the (possibly partially corrupted) code word (Yekhanin, 2006). W-H codes are mathematically orthogonal codes, so when using perfect synchronization they can only cross-correlate with themselves, thereby eliminating multi-access interference. Examples of W-H codes are shown in figure 2.8.

There are a number of drawbacks for use of these sequences in CDMA. The codes can have multiple autocorrelation peaks, making external synchronization necessary. Partial sequence cross-correlation can also be non-zero, enabling multipath interference and losing the advantages of the use of orthogonal codes (Meel, 1999).

$$H1 = \begin{pmatrix} 0 & 0 \\ 0 & 1 \end{pmatrix}$$

$$H2 = \begin{pmatrix} 0 & 0 & 0 & 0 \\ 0 & 1 & 0 & 1 \\ 0 & 0 & 1 & 1 \\ 0 & 1 & 1 & 0 \end{pmatrix}$$

$$H3 = \begin{pmatrix} 0 & 0 & 0 & 0 & 0 & 0 & 0 & 0 \\ 0 & 1 & 0 & 1 & 0 & 1 & 0 & 1 \\ 0 & 0 & 1 & 1 & 0 & 0 & 1 & 1 \\ 0 & 1 & 1 & 0 & 0 & 1 & 1 & 0 \\ 0 & 0 & 0 & 0 & 1 & 1 & 1 & 1 \\ 0 & 1 & 0 & 1 & 1 & 0 & 1 & 0 \\ 0 & 0 & 1 & 1 & 1 & 1 & 0 & 0 \\ 0 & 1 & 1 & 0 & 1 & 0 & 0 & 1 \end{pmatrix}$$

Figure 2.8: Examples of Walsh-Hadamard (W-H) codes. Three Hadamard matrices are shown, from which W-H codes can be created. The first matrix (H1) provides two W-H codes of length two; 00 and 01, the second (H1) provides 4 codes; 0000 0101 0011 0110. All codes created using a Hadamard matrix are orthogonal to each other.
[From: (Langton, 2002), page 8]

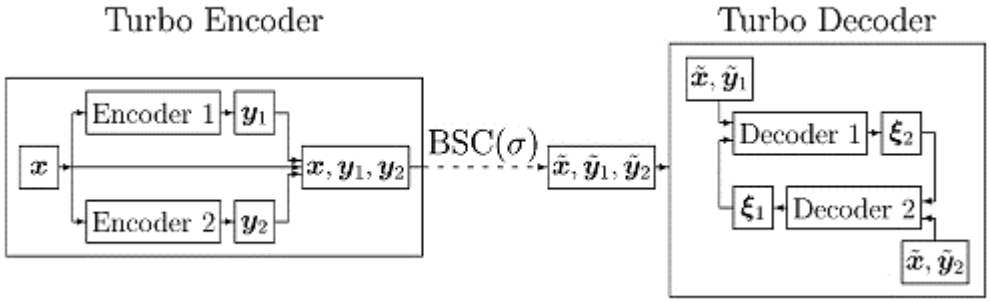

Figure 2.9: Structure of Turbo codes. The code word *x* is encoded by two different encoders and the original code word is send with the two ciphered versions. The receiver uses two decoders, one inferring the original bits from (x, y_1) and the other from (x, y_2). When the decoded bits do not match probabilistic information about each bit (ξ_1 and ξ_2) is exchanged between the decoders. This is done in an iterative process until the two bits match.
[From: (Ikeda, Tanaka, & Amari, 2004), figure 1]

Table 2.1: Known Barker Codes

Length	Code
2	+-, ++
3	++-
4	+-++, +---
5	+++-+
7	+++--+-
11	+++---+--+-
13	+++++--++-+-+

Table 2.1: Known Barker Codes. Only eight Barker codes are known (Borwein & Mossinghoff, 2008), it is postulated that no more Barker codes exist (D Terr, 2012).

$$\mathbf{H} = \begin{bmatrix} 0 & 1 & 0 & 1 & 1 & 0 & 0 & 1 \\ 1 & 1 & 1 & 0 & 0 & 1 & 0 & 0 \\ 0 & 0 & 1 & 0 & 0 & 1 & 1 & 1 \\ 1 & 0 & 0 & 1 & 1 & 0 & 1 & 0 \end{bmatrix}$$

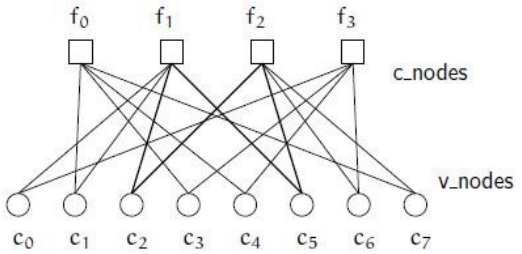

Figure 2.10: A Low-density parity-check (LDPC) code. The top shows the sparse parity-check matrix. It is called sparse or low density, as there are only a few 1's as compared to the number of 0's. The bottom half shows the corresponding bipartite (Tanner) representation of the matrix.
[From: (Leiner, 2005)]

- ***Turbo codes***

Turbo codes are a class of convolutional codes whose performance in terms of Bit Error Rate (BER) are close to the Shannon–Hartley limit, the theoretical maximum rate of information transmission over a noisy channel (Berrou, Glavieux, & Thitimajshima, 1993; Le Goff, Glavieux, & Berrou, 1994). The turbo code (figure 2.9) consists of the original message *x* and the (parallel) concatenation of two convolutional codes (y_1, y_2). After reception, the different parts of the turbo code are decoded using two different decoders, one inferring the original bits from (x, y_1) and the other from (x, y_2). If the infers differ, soft (probabilistic) information about each bit (extrinsic variables ξ_1 and ξ_2) is exchanged between the two decoders in an iterative fashion, until both decoders give the same decision with the same probability about each symbol (Ryan, 1998).

Since the description of the first Turbo code, the parallel concatenated convolutional code (PCCC), many other classes of turbo codes have been introduced, including serial versions and repeat-accumulate codes (Benedetto & Montorsi, 1996; Divsalar, Jin, & McEliece, 1998; Jin, Khandekar, & McEliece, 2000).

- ***Low-density parity-check codes***

Low-density parity-check codes (LDPC codes) are linear codes obtained from sparse bipartite graphs. The code is described by its (sparse) parity-check matrix, which can be efficiently represented by a bipartite (Tanner) graph (Gallager, 1962). Figure 2.10 shows an example of a graph with f left nodes (variable nodes) and c right nodes (check nodes), giving rise to a linear code of block length f and dimension $c - f$.

A number of distinct methods for constructing LDPC's have been proposed, differing in code length, encoder/decoder complexity and performance (Chung, Richardson, & Urbanke, 2001; Fossorier, 2004; Hou, Siegel, & Milstein, 2001; Z. Li, Chen, Zeng, Lin, & Fong, 2006; Luby, Mitzenmacher, Shokrollahi, & Spielman, 2001; T. J. Richardson, Shokrollahi, & Urbanke, 2001). Like turbo codes, LDPC codes have near-channel-capacity error correction. Using a sufficiently long enough code word length, they can operate within a fraction (a few milli-dB) of the capacity limit (Chung, Forney Jr, Richardson, & Urbanke, 2001).

Turbo codes and LDPC codes have found their use in providing reliable information transfer in bandwidth- and latency-constrained communication in noisy environments, like (deep space) satellite communication and high-speed telecommunication. Both types of code have an “error-floor”, at very low SNR-levels the BER curve flattens and their performance doesn’t improve much (T. Richardson, 2003). They provide similar performance, although LDPC has a lower decoding complexity (Oksman & Galli, 2009).

Spread spectrum stimuli as possible tool for neuroscience

Consider the brain as a noisy channel information processing system with noisy-channel characteristics. Presentation of a stimulus to the brain, using one of the sensory systems as input, evokes brain activity of some sort which can be measured using brain imaging techniques like EEG. Spread spectrum signal transmission and the CDMA codes used herein offer a number of possibilities for use as stimuli in neurological research, as these signals were selected for their convenient properties when used in noisy environments. Spreading the signal might circumvent frequency bound (narrowband) interference from internal processes like spontaneous brain oscillations or sensory encoding limitations. Their correlation properties are useful when offering multiple stimuli simultaneously.

An important assumption is that the brain response to a noise-tagged stimulus is an attenuated, time-lagged version of the stimulus, since then the tagged stimuli can be detected using a simple correlation approach (Farquhar, Blankespoor, Vlek, & Desain, 2008). Distortion of the signal shape by sensory or cognitive processing does not have to pose a problem, for as long as the operations performed by the brain follow a linear path, this can be overcome by adding some sort of training session for automatic pattern recognition. Of course this linearity is a very coarse and for large parts of the brain probably inaccurate requirement, but for some of the simpler sensory systems it might hold. Desain (2008) has shown assuring results with the estimation of the impulse response to the first derivative of noise tagged auditory stimuli, wherein training of the classifier was only needed for responses of one stimulus class and a limited number of trials.

Spread spectrum in neurophysiologic research

Pseudorandom sequences such as m-sequences are regularly used to randomize stimulus presentation (i.e. (Buracas & Boynton, 2002; Jia, Smith, & Kohn, 2011; Katzner et al., 2009; Lacey, Stilla, & Sathian, 2012)), but this can hardly be classified as spread spectrum, as the stimuli themselves are not spread out over a larger frequency range. However, spread spectrum stimuli have been employed as well. Pseudorandom noise sequences have been used to in as input for single cell behaviour to produce estimates of linear system unit impulse responses (UIRs) (Marmarelis & Marmarelis, 1978; Møller, 1977; Møller & Jannetta, 1983; Møller & Rees, 1986; Møller, 1986; Møller, 1987; Møller & Angelo, 1988; Møller & Jho, 1989; O'Leary & Honrubia, 1975) and non-linear system unit impulse responses (Shi & Hecox, 1991).

Pseudorandom noise is applied to probe auditory memory since a long time (Guttman & Julesz, 1963; Julesz & Guttman, 1963), for an overview see (Agus, Thorpe, & Pressnitzer, 2010). For characterization and evaluation of hearing-loss a long session of presenting one by one a stimulus at a specific frequency and determining loudness threshold is necessary. This is cumbersome, especially in babies, and the use of various kinds of spread spectrum stimulation is an active field of research (Z. Chen, Hu, Glasberg, & Moore, 2011; Supin, 2008; Supin, 2011).

Stimuli with a repetitive character give strong responses in EEG and MEG measurements in auditory, tactile and visual domains, the so called Steady State Evoked Potentials (SSEP). It is postulated that the periodic stimulation induces frequency- and phase-locking responses in neural circuits, provoking the SSEP (Regan, 1977). This hypothesis could be tested by using spread spectrum techniques; by spreading the stimuli over different frequency- and phase-bandwidths the (existence of) limits of these responses could be found.

Spread spectrum and error correcting coding in brain computer interfaces

SSEPs are used a lot in EEG/MEG-based BCI systems, as they give clearly distinguishable responses in a narrow frequency band and multiple tags can be used simultaneous due to the uncorrelated nature of different frequencies (Farquhar et al., 2008), but also suffer from some drawbacks. The frequency domains used for SSEPs are in the same range (10-140Hz) as spontaneous brain oscillations, acting as a big source of noise. The processing gain obtained by using spread spectrum techniques can circumvent this problem. However, this would only work if the underlying hypothesis of the attenuating process of SSEP does not hold: oscillators cannot attune to non-periodic or fast changing signals (Desain, Farquhar, Blankespoor, & Gielen, 2008).

In designing a BCI with codes attached to the various stimuli (like in a P300 speller) one can take the route of either designing noise sequences with proper characteristics to allow for easy decoding. Here the multi-user access techniques mentioned could be beneficial, as increasing the number of stimuli that can be offered simultaneously and without cross-interference, can help increase decisions-rates and thereby information transfer rates in attention- and decision-based BCI systems. Or one could conceptualize the system as a transmission line in which a symbol (a code from a codebook) is transmitted and the received bit-sequence may contain errors. In that case redundant or error-correcting codes can be used that trade code-length for robustness: it is not likely a single or a few errors will make the code be interpreted as a different symbol, as the codes are chosen to have a large enough (Hamming) distance.

For P300 spellers the code-book describing which letters to flash at any given point in the sequence have been optimized using codes with large hamming distances (Hill, Farquhar, Martens, Bießmann, & Schölkopf, 2009; Martens, Hill, Farquhar, & Schölkopf, 2007; Martens, Hill, Farquhar, & Schölkopf, 2009). In this process other characteristics of the perceptual system (like the refractory period of p300 response) got in the way to achieve very large improvements. Optimizing for maximal Hamming distance criterions lead to an overall increase in target frequency of target stimuli, and thereby to a significant reduction in target-to-target intervals. This gave an overlap in event-related potentials (ERPs), making classification of these ERPs much more difficult (Hill et al., 2009). Combination of this codebook approach with stimuli flashing in a pseudorandom controlled manner, the low cross-correlation properties could make the identification of the ERPs less troublesome.

A small number of studies in BCI have been performed using spread spectrum techniques and/or the code sequences mentioned in this thesis. In the introduction of this thesis (chapter 1) c-VEP was already mentioned as an example of a promising stimulus sequence design. In the next chapter two auditory methods will be examined and in the 4th chapter multiple visual methods will reviewed.

CHAPTER 3 – AUDITORY BCI-EXPERIMENTS USING CONTINUOUS AND BINARY NOISE TAGS

A small number of auditory brain computer interface experiments using spread spectrum stimuli have been published. Two methods are applied in these articles, the auditory-evoked spread spectrum analysis (AESPA) method and the noise-tagging method. Both methods will be explained here, and, as far as possible, a comparison between the two methods will be made, noting important similarities and differences.

Tagging with continuous Gaussian noise: Auditory-Evoked Spread Spectrum Analysis (AESPA) [1]

The group at the Trinity College Institute of Neuroscience, Dublin, Ireland, headed by John J. Foxe published a number of articles in which they use their auditory-evoked spread spectrum analysis (AESPA) method, which is the auditory equivalent of their VESPA technique. This method used Gaussian noise signals to amplitude-modify a broadband noise carrier wave, and is based on the assumption that the output EEG consists of a convolution of this input signal *x(t)*, with an unknown impulse response *w(t)* plus noise (figure 3.1). This unknown impulse response is termed the AESPA and is obtained by performing a linear least squares estimation using the known audio amplitude modulation signal and the measured EEG. The AESPA response thus can be considered analogous to a filter describing the brain transformation from auditory input into EEG output (A. J. Power, Reilly, & Lalor, 2011).

After introducing their method (A. J. Power, Lalor, & Reilly, 2007), comparing it with standard-technique auditory evoked potentials (AEPs) (J. Foxe, Lalor, Power, & Reilly, 2009), showing the possibility to measure two simultaneously and binaurally presented stimuli using AESPA (A. J. Power, Lalor, & Reilly, 2009), and extending the linear AESPA model with a quadratic model (A. J. Power et al., 2011), they put AESPA to more practical use. They use it to obtain temporally detailed responses to natural speech stimuli (E. C. Lalor & Foxe, 2010), investigate effects of endogenous attention on sensory processing in the auditory system (A. J. Power, Lalor, & Reilly, 2011), and attentional effect on exogenous stimulus processing in a natural, cocktail-party-like setting (A. J. Power, Foxe, Forde, Reilly, & Lalor, 2012).

Explanation AESPA

For most of these papers the experimental setup is standardized; the EEG acquisition, stimuli used and the signal processing (AESPA estimation) are the same, only the number of participants, the task performed and quantification of the results are modified to accommodate the research question. Figure 3.2 shows an overview of the AESPA acquisition. The stimulus consists of a Gaussian broadband noise carrier wave with energy limited to a bandwidth of 0-22.05kHz[2], amplitude-modulated by Gaussian noise signals with uniform power in the range of 0-30Hz. For a more linear perception of the audio intensity modulation, the values of these modulating signals are mapped using an exponential relationship accounting for the logarithmic nature of auditory stimulus intensity perception.

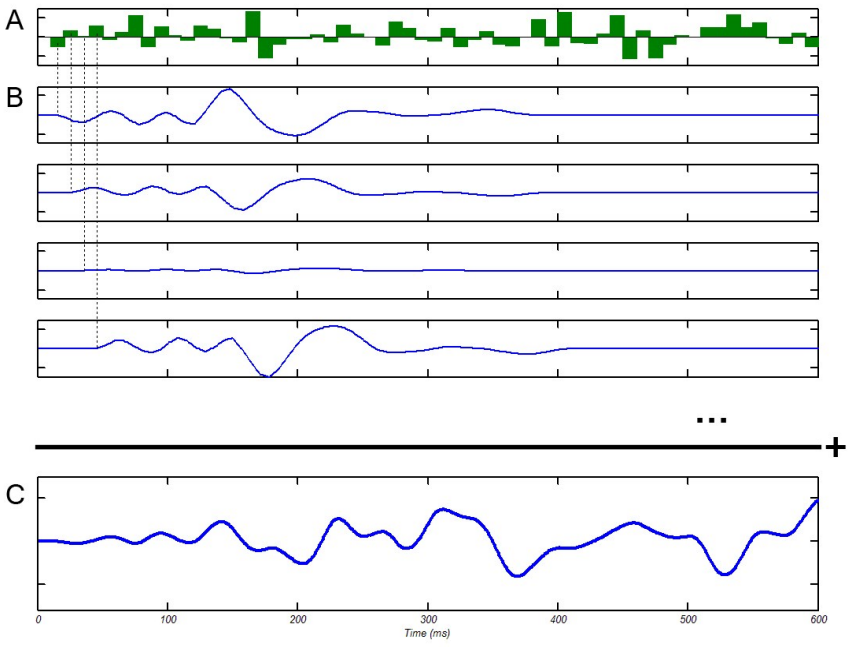

Figure 3.1: Decomposition of the impulse response into its structural components. In (A) a Gaussian noise stimulus is shown. Each discrete pulse of the stimulus evokes an (scaled and time-shifted) impulse response (B). The total impulse response is a convolution of all of the single impulse responses (C).

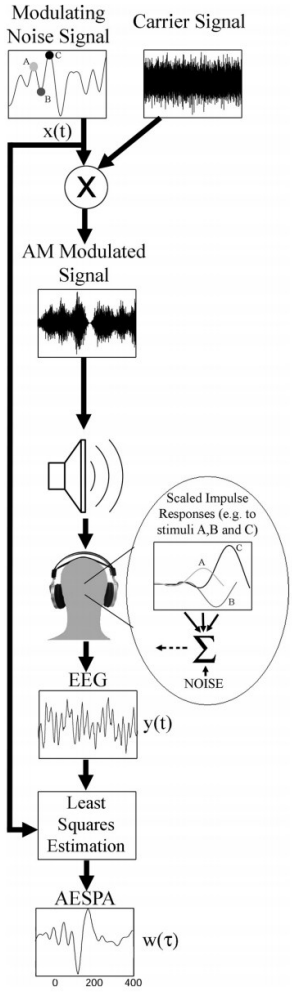

Figure 3.2: Flow diagram of auditory-evoked spread spectrum analysis (AESPA) acquisition. [From: (J. Foxe et al., 2009) - figure 2]

During experiments participants are asked to minimize any muscle movements, as even short blinks can have a detrimental effect on the measurement. EEG data is recorded using 130 electrodes[3], filtered for the range 0-134Hz. The stimulus delivery and recorded EEG data are synchronized. EEG data were then digitally band-pass filtered (offline) between 2Hz and 35Hz. The AESPA is obtained by performing a linear least squares estimation, using a sliding window from 200 ms pre-stimulus to 400 ms post-stimulus, advanced sample by sample. Each time point gives the relative time between the continuous input intensity signal and the continuous EEG, wherein the relationship between these two is expected to be zero for times before t=0, but can be positive for time points after the stimulus delivery, depending on the cognitive speed and the electrode site.

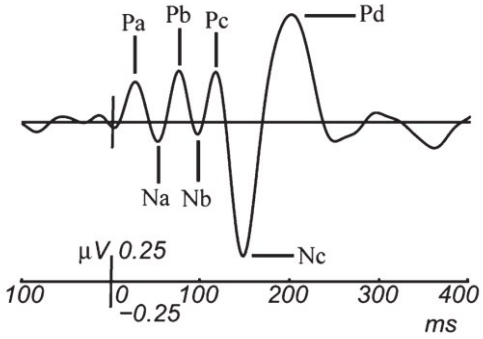

Figure 3.3: A typical AESPA response, obtained at Fz using a modulated broadband noise carrier in the range 0-22.05 kHz. The response shows several distinct components, which are labelled in an AEP-like fashion. [From: (A. J. Power et al., 2011) - figure 1]

A typical AESPA response is shown in figure 3.3. In general AESPA yielded lower signal-to-noise ratios than the standard AEP, but the measured responses showed considerable correlation to the standard AEP. High SNR values could be achieved at specific channel locations (A. J. Power et al., 2007). Like an AEP, the AESPA response shows several distinct components, although the morphology is distinctly different. Foxe and Lalor (2009) give an in-depth comparison of AEP and AESPA, as well as their specific components, and they consider the standard AEP as a special case of the broader AESPA method. At last, a quantification of the results is conducted, often focusing on a specific component of the AESPA signal (i.e. Nc or Pd), but as this depends on the specific tasks performed, it will not be discussed here further.

Potential AESPA

The AESPA method has been shown a useful procedure to model the responses of the auditory system to novel stimuli. Correlation tests have found statistically significant predictive power, although correlation values acquired were not remarkably high and signal-to-noise ratios were lower than for the standard AEP, which is explained by the noisy nature of EEG signals (A. J. Power et al., 2007; A. J. Power et al., 2011). Incorporating second and higher orders in the modelling has shown small, but significant improvements on the predictability of the model (A. J. Power et al., 2011). This approach can help include some of the non-linear processing known to be performed in the auditory system, for example in intensity mapping (Green, 1988).

Tagging with binary pseudo random noise

The group at the Nijmegen Institute for Cognition and Information at the Radboud University Nijmegen, Netherlands headed by Peter Desain propose a direct sequence spread spectrum based alternative for steady state stimulus tagging. In a preliminary EEG experiment the feasibility of this method for both perceptual and selective attention based BCI-systems is shown (Farquhar et al., 2008), while a second paper focuses more on the classification and structural decomposition (convolution) of the noise codes (Desain et al., 2008).

Explanation Noise-Tagging

In noise-tagging a saw-tooth wave carrier signal is amplitude-modified by multiplying it with a Gold code[4], with a modulation depth of 80% (i.e. reducing the amplitude to 20% for the 0-bits of the Gold-code). This stimulus is delivered in blocks containing multiple epochs of this sequence. Under the assumption that the brain response is an attenuated, time-shifted version of the stimulus, as a first approach they detect the noise tag using a simple correlation approach. EEG data is recorded using 256 electrodes[5], sampled at 2048Hz, but down sampled to 512Hz, as no brain signals were expected above 256 Hz. EEG data were then digitally filtered (offline) using a band-pass filter (30-80Hz).

An estimation of the impulse-response for each single up or downward edge in the binary stimulus, obtained by using a least-squares technique, is then used to reconstruct the total response to the known overlapping stimulus sequence, and this estimated sequence is correlated with the measured EEG signal as basis for the classification. This is illustrated in figure 3.4, each up or downward edge causes a time-shifted version of the response. These are summed to arrive at the predicted output.

The use of Gold-sequences as stimulus modulator is an requisite for a successful convolution, as the convenient correlation characteristics of these sequences ensure both minimal temporal aliasing between overlapping epochs (due to the low autocorrelation properties) and minimal interference between different tags (due to the low cross-correlation).

Potential noise-tagging experiments

The experiments confirmed the feasibility to extract noise tagged stimuli from EEG signals on a single trial basis, including identification of the presented tag, neural time lag and effect of selective attention (Farquhar et al., 2008). Presentation of multiple simultaneous stimuli in a selective attention task, essential for selective attention BCI-systems, gave comparable results to those of frequency tagging (Blankespoor, 2008). A big advantage is that training of the classifier is only necessary for impulse-responses of one stimulus class, which then can also be used for other stimulus classes, limiting training times to about one minute (Desain et al., 2008).

Comparison of the two methods

Basic assumption

Both the AESPA method as the noise-tagging method are based on the assumption that the stimulus is made of a combination of simple components (pulses of varying amplitude or positive or negative edges) and the EEG response to a full stimulus is made out of a combination of attenuated, time-shifted responses to that basic stimulus component (figure 3.1). The parameters of this 'impulse response' can be recovered using a least-squares regression (figure 3.4) (Desain et al., 2008; A. J. Power et al., 2011).

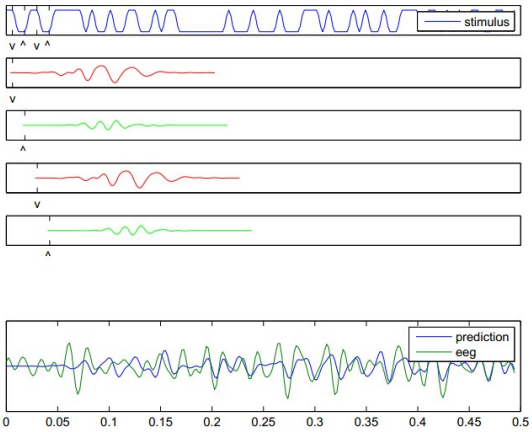

Figure 3.4: Decomposition of the impulse response into its structural components (top) and fit to the data (below). Note that different responses to rising (0-1) and falling (1-0) transitions are postulated in this model. [From: (Desain et al., 2008) - figure 2]

Modulation sequence

The noise-tagging method uses binary Gold-sequences to modulate their signals, as these codes form complete sets of sequences with known and favourable correlation properties. AESPA uses Gaussian noise signals to modulate a Gaussian broadband noise waveform, from which signals with the desired statistical properties were selected. Which properties they desire and how this selection is performed is not specified, but these can be anticipated to be alike the properties of the noise-tagged signals. AESPA (like its visual counterpart VESPA) uses Gaussian signals to modulate the stimuli, as the resulting estimated impulse responses are expected to be sharper and be more sensitive to changes in brain state and function, manifesting in the VESPA having more structure, narrower peaks and higher between-subject variability than when binary stimuli are used (E. C. Lalor, Pearlmutter, Reilly, McDarby, & Foxe, 2006).

Frequency range

AESPA focuses on the frequency band between 2-35Hz, where noise-tagging focuses on the band between 30-80Hz. Power & Lalor advocate the AESPA frequency band range pointing out that the EEG power above 30 Hz is typically very low (A. J. Power et al., 2007). In the noise-tagging experiments the chosen band-pass gave some improvement over non-band-passed data and other band passing widths, but the choice for this range seems mostly influenced by the improvements it gave in the analysis of the frequency tagging data part of their experiment (Blankespoor, 2008). In their later experiments, Power et al (2012) use the amplitude-envelope of natural speech as stimulus for their AESPA method. Here a low pass filter (<20Hz) is applied, as the envelope frequencies between 2 and 16 Hz provide strongest effects on speech-intelligibility (Drullman, Festen, & Plomp, 1994a; Drullman, Festen, & Plomp, 1994b; A. J. Power et al., 2012).

Effects of selective attention on methods

Both groups have tested their method in an attention based setting. In (Farquhar et al., 2008) two different tagged stimuli were presented, one to each ear, and participants had to selectively attend to one of the tags by a simple counting task. Above-chance-level results were found for some of the participants, however, they did not find consistent results across subjects. This could be due to the low number of participants and difficulty of the attentional task condition, as the noise-tagged stimuli gave comparable results to the frequency tagged stimuli in this task. Power et al. (2009) showed the ability of AESPA to extract responses to two simultaneously presented stimuli, as well as a modulation effect of auditory attention, giving a stronger SNR for the attended stream, resulting in a higher obtained AESPA. This is in support of the gain/filter theory of auditory attention (Hillyard, Hink, Schwent, & Picton, 1973; A. J. Power et al., 2009). These results were confirmed by subsequent experiments, which used the AESPA method to further investigate endogenous auditory attention (A. J. Power et al., 2011) and attentional effects on exogenous stimuli (A. J. Power et al., 2012) in a cocktail-party like setting.

NOTES

[1] Unless noted otherwise, the information in the next six paragraphs is gathered from (A. J. Power et al., 2007)

[2] In (A. J. Power et al., 2007) a 2 kHz pure tone carrier wave is also modulated using the spread spectrum signals, but did not result in any appreciable AEP-like responses. In (A. J. Power et al., 2011) two root mean square normalized band-pass noise carriers of 1 kHz bandwidth centered at 1 kHz and 5 kHz are employed. In (A. J. Power et al., 2012) (the amplitude-envelope of) natural speech is used as stimulus.

[3] In (A. J. Power et al., 2007) 128 electrode positions are used. In (A. J. Power et al., 2012) 34 participants were measured using 130 electrodes, 6 participants were measured using 162 electrode positions. The responses extracted from the data of these 6 were mapped down to the 130 positions using a spline interpolation algorithm.

[4] In (Farquhar et al., 2008) two saw-tooth carrier signals of 512 and 768 Hz are modified using a 255-bits Gold-code (128 bits/sec modulation rate; 2 second epoch). In (Desain et al., 2008) a 420 Hz saw-tooth carrier wave is AM modulated using a Gold-code (bit length unknown, 168 bits/sec modulation rate; epoch length unknown). In both experiments the modulation signals were smoothed using a cosine filtered, so the transition between a zero and one looks like a sine wave segment.

[5] In (Desain et al., 2008) a 128 channel EEG response was recorded.

CHAPTER 4 – VISUAL BCI-EXPERIMENTS USING CONTINUOUS AND BINARY NOISE TAGS

Multiple groups have used spread spectrum stimuli in brain computer interface experiments. In the first chapter the pseudorandom code modulated visual evoked potential (c-VEP) was already mentioned. Here a pseudorandom binary sequence is used to elicit VEPs. This method was first explored by E.E. Sutter and subsequently a number of groups have used variations of this method under diverse names, producing mixed results. A second method is the visually evoked spread spectrum response potential (VESPA), using Gaussian noise waveforms instead of binary sequences. As in the previous chapter, the different methods will be described and compared.

Tagging with binary pseudo random noise: *Erich E. Sutter – Multifocal m-sequence technique*

Erich E. Sutter of the Smith-Kettlewell Eye Research Institute was the first who suggested using a single, time-shifted, pseudorandom binary sequence in a simultaneous stimulation BCI scheme (E. E. Sutter, 1992). Sutter previously developed a multifocal technique for electroretinography (mfERG), where different retinal areas are stimulated simultaneously using elements controlled by time-shifted versions of an m-sequence. Electrodes placed on the cornea and the skin near the eye measure the electrical responses of various cell-types in the retina. Cross-correlation between the m-sequence for a particular area and the single raw trace recording gives the independent multifocal ERG responses (E. Sutter, 1985). The mfERG has become an indispensable tool in electrophysiology and electroretinography (for reviews, see (Lai et al., 2007; Parks, Keating, & Evans, 2002)). In his 1992 paper Sutter tried to use this method in a communication device for locked-in patients by offering multiple stimuli simultaneously and letting the patient choose one by fixating on it. As the area around the fovea contains the highest density of light receptors, the element covering the centre of the visual field generates the largest contribution to the ERG signal. However, ERG did not prove practical for this approach; the ERG signal is too small, requiring long average time; measurement of high quality ERG requires direct contact with the cornea; blinks and eye movements generate enormous artefacts. By extending his method to visual evoked potentials[1] these inconveniences could be diverted, as the VEPs are measured using non-invasive EEG, which also suffers from artefacts from blinks and eye movements but at a lower level. Magnification of the centre of the visual field is further amplified between the receptors (cones) and the ganglion cells, resulting in additional enhancement of the centre of the visual field, a process known as cortical magnification. This is helpful in distinguishing attended from unattended stimuli, as the attended stimuli will give a stronger response.

As in mfERG, the mfVEP method uses binary m-sequences to moderate targets' flash frequencies. Binary stimuli are used since they can be implemented using relatively simple and inexpensive display technology. Pseudorandom sequences are applied, as these offer a high level of orthogonally, giving little to no correlation between the sequences of the different targets, facilitating identification of the used code in the measured response. M-sequences abide these requirements, and if different time-shifted versions of one m-sequence are used, all sequences have a high level of equivalence. Target stimuli are 64 rectangular fields displayed as an 8x8 matrix. Due to cortical magnification the main response measured by the EEG is the contribution of the fixated field and its immediate neighbours, making the response cycle independent for the fixated target except for a shift shaped by the lag in the sequence of the fixed field. At the borders a wrap-around technique is applied in order to achieve equivalence of all target fields, i.e. every target is surrounded by border fields (figure 4.1). The modulation rate of the m-sequence is imposed by the frame rate of the display used, in Sutter's experiment a frame rate between 40 and 70 frames/s, and 8 samples/frame was used.

	57	*58*	*59*	*60*	*61*	*62*	*63*	*64*	1
64	1	2	3	4	5	6	7	8	9
8	9	10	11	12	13	14	15	16	17
16	17	18	19	20	21	22	23	24	25
24	25	26	27	28	29	30	31	32	33
32	33	34	35	36	37	38	39	40	41
40	41	42	43	44	45	46	47	48	49
48	49	50	51	52	53	54	55	56	57
56	57	58	59	60	61	62	63	64	1
64	1	2	3	4	5	6	7	8	9

Figure 4.1: Stimulus presentation (64 rectangular fields) displayed as an 8 x 8 matrix using wrap around technique. Lags in simulation of the different fields increases from left to right in each row and from top row to bottom row. Wrap around accomplishes that every target is surrounded by an equal number of neighbour fields, ensuring equivalence of the target stimuli. Numbers in italic correspond to fields of the preceding frame, underlined numbers to those of the next frame. [From: (E. E. Sutter, 1992) - figure 2]

The measured EEG response is cross-correlated with the estimated response wave for all possible targets, and these correlation coefficients are compared with each other as well as a threshold value. The highest coefficient which remains above threshold for a certain time is selected as the attended target. The used threshold value can be adapted on the fly to the strength of the signal, avoiding erroneous responses during periods of excessive noise. An estimation of the response amplitude is constructed using the raw signal and the recorded raw response template. As a time-shifted version of the same m-sequence is used for all targets, the same response template can be used for all targets by shifting it with the corresponding lag, simplifying the real-time calculations required.

The technique was implemented in a prototype integrated BCI system capable of producing high quality synthetic speech, word processing on a personal computer and accessing applications. A matrix of 64 rectangular labelled fields (keys) with 32 levels of key

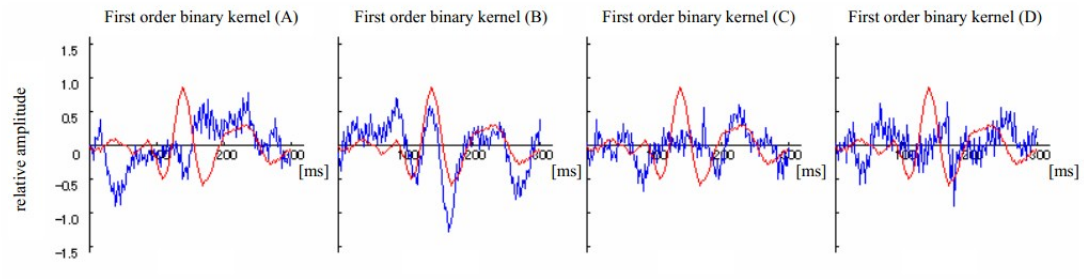

Figure 4.2: Kernels obtained from a subject as he observed target (answer) "B".
Each kernel (blue line) is calculated by cross correlating the PRBS used as stimulus ("A", "B", "C" and "D") with the measured VEP. The kernel resembling the subjects reference kernel (red line) the most is picked as the attended target.
[From: (K. Momose, 2007) - figure 2]

functions offered a total of 2048 programmable key functions, i.e. letters, words, sentences and controls for special devices. The prototype was tested with 70 normal subjects and approximately 20 severely disabled persons. After an initial training process lasting 10 minutes up to one hour, adequate response times between 1 to 3 seconds were reached within the normal subjects. Significant between-subject variations in optimal stimulation mode and rate were found, although some general notions could be made: Colour alternation between equiluminant red and green were almost as effective as flickering targets, while being much less tiring for the subjects, with fine red/green check pattern reversals giving strongest performance. In disabled persons two hindrances for extensive, daily usage were experienced. The two most common disabilities among patients inclined to use BCI-systems, cerebral palsy and amyotrophic lateral sclerosis, often cause EEG artefacts originating from involuntary muscle movement, mainly from the neck musculature. Also performance of the system depended on good placement and maintenance of the electrodes, requiring adequately trained nursing staff. To circumvent these problems, one ALS patient had intra-cranial electrodes implanted, which resulted in 5-10 times larger responses and decreased artefacts from muscle movement. Transcutaneous electrode strips are invasive, presenting a small risk of infection that could result in meningitis. In this subject the implanted electrodes did not cause any discomfort except a short initial healing process, and electrode impendence and signal quality remained stable for the entire evaluation period of 11 months. Toward the end of this period the subject reached communication rates of 10-12 words/minute (ITR of 100>bits/min), could operate his gaze-addressable keyboard with an access time of 1.2s and was able to control his television set and VCR without help. These rather good results in a patient as reported by (E. E. Sutter, 1992) have not been replicated by others.

Momose et al. - Eye gaze point detection system using pseudorandom stimulation for BCI

K. Momose from the Faculty of Human Sciences, Waseda University, Japan, presented a prototype BCI system using pseudorandom binary sequence elicited VEP (K. Momose, 2007). His system is based on the principles of Sutter's paper from 1992 described above and uses the first order cross-correlation functions (kernels) to resolve the fixated target. Healthy subjects (n=3) were presented an easy question and had to answer by fixating one of four simultaneously presented choices. Each answer was luminance modulated by a different m-sequence, obtained from a 9-bit shift register with a clock of 100Hz. The answers were presented for about 5 s. EEG recordings were taken with 10-20 electrodes at O_Z and C_Z. During the test experiment, each subject was presented 12 questions. A short training experiment with a PRBS stimulation of about 40 s was performed before the test experiment to measure the subject's reference kernel.

Figure 4.2 shows an example of kernels obtained from one subject. In this case the subject observed target "B", which was correctly determined from the highest coefficients. Gazed target were obtained within 6s (ITR of 10 bits/min) with a mean error rate of 22%, demonstrating the fundamental validity and effectiveness of the system to detect gazed target. Low concentration of subjects during target fixation and unstable kernel estimation increased the error rate, making the current system insufficient for practical use, but improvement and optimization of kernel estimation and classification method could address these nuisances.

Shangkai Gao et al. - Pseudorandom binary sequences modulated visual evoked potential

In 2009 the group of Shangkai Gao at the Tsinghua University, China, compared a c-VEP BCI with a frequency modulated VEP BCI (Bin et al., 2009). Their c-VEP BCI system is also based on the system of Sutter (1992). A 63 elements binary m-sequence was used as modulation signal for 16 rectangular stimulation targets, displayed on a 4x4 matrix using a wrap-around principle as in figure 4.1. Time lags of the different targets were separated by 4 time steps from the previous block for each stimulus block (figure 4.3a). EEG was captured using a SynAmps2 system (NeuroScan) at 1000Hz from 47 electrodes, using electrode O_Z as signal channel and a variable bipolar reference channel. In a training experiment the subject had to fixate one of the targets so a template could be obtained and the channel with the maximized training accuracy could be selected as the optimal reference channel. During the testing phase of the experiment the 20 healthy subjects were asked to enter two strings of 32 characters using the BCI system. The neuronal response evoked by the pseudorandom stimulus had a broadband spectrum distributed over 5-25Hz (figure 4.3c). The average training accuracy found was 95±6%, the online accuracy was 91% and the ITR was 92.8±14.1 bits/min, all of them higher than the f-VEP BCI system tested for comparison.

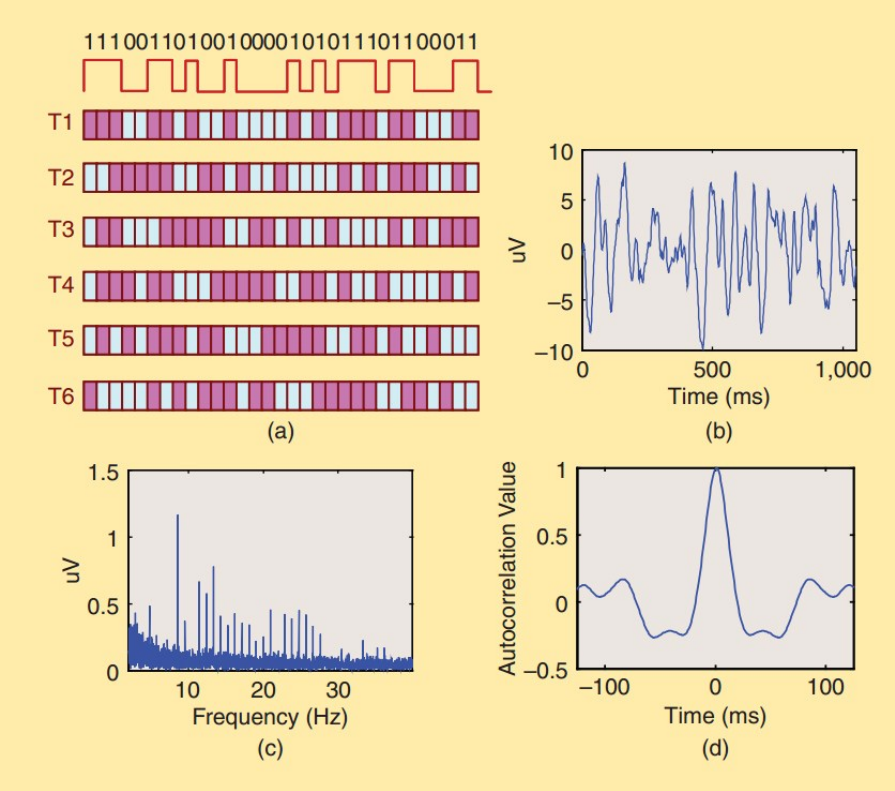

Figure 4.3: Stimulus sequences and evoked response of Goa's c-VEP system.
a) Sequences of targets in one stimulation cycle, with a four-frame lag between consecutive sequences.
b) Waveform of the evoked response.
c) Power spectrum of the evoked response.
d) Auto-correlation function of the evoked response.
[From: (Bin et al., 2009) - figure 4]

A year later Yun Li at the same group used this method to investigate the time required for information conduction across the corpus callosum, the interhemispheric transfer time (IHTT). Here he used the same stimulus setup as above, with only one notable deviation; EEG signals were pre-processed by band pass filtering (1-40 Hz) and averaged over 200 trials. Results showed the feasibility of the use of m-sequence coded VEPs to investigate the IHTT, yielding more robust results with higher performance than the traditional flash VEP methods (Y. Li, Bin, Hong, & Gao, 2010).
In 2011 an improved version of their c-VEP BCI system was presented, using 32 targets instead of 16 and a multichannel identification method based on canonical correlation analysis (CCA) as target classifier. Except for these differences, the stimulus setup was kept alike the previous system. Training stage required subject to fixate a reference target for 200 stimulus periods (approximately 3.5 min), in the testing stage the subject had to enter a sequence of 64 characters. The system reached an average ITR of 108±12 bits/min (over 5 subjects), with one subject reaching 123 bits/min (Bin et al., 2011).

Nezamfar et al. - VEPs induced by multiple pseudorandom binary sequences
The Cognitive Systems Laboratory of the Northeastern University, Boston, USA, in collaboration with a group at the Oregon Health and Science University, Portland, USA published two papers in 2011 presenting results from their initial studies using m-sequences as stimuli for a BCI system (Nezamfar, Orhan, Erdogmus et al., 2011; Nezamfar, Orhan, Purwar et al., 2011). In contrast to the previously discussed visual BCI systems, Nezamfar et al used multiple different m-sequences instead of shifted versions of the same m-sequence. This offers the advantage that precise timing information of the stimuli is not required for the signal processing and detector algorithms, as contrasted to when shifted versions of one m-sequence are used. However in both experiments timing information is still assumed, such that the basic template matching classifiers as employed by (Bin et al., 2009) can be applied. The main goals of their experiments are to test a naïve Bayesian fusion classifier against the basic classifier (Nezamfar, Orhan, Purwar et al., 2011) and to investigate the effect of different bit presentation rates on the VEP classification rate (Nezamfar, Orhan, Erdogmus et al., 2011; Nezamfar, Orhan, Purwar et al., 2011).

The stimulus are two inverted 10x10 checkerboard patterns, with the flashing sequence determined by one of four 31-bits m-sequence with a modulation rate of either 15 or 30Hz. The 4 different m-sequences were selected from the among all 31-length m-sequences minimizing the pair wise cross-correlations. Healthy subjects (n=5 (Nezamfar, Orhan, Purwar et al., 2011) and n=2 (Nezamfar, Orhan, Erdogmus et al., 2011)) participated in two sessions, during each session one of the two modulation rates was used, and the subject was presented 80 trials, 12 of each m-sequence. EEG signals were captured using 16 electrodes at sites having higher spatial density around the visual cortex.

Results from (Nezamfar, Orhan, Purwar et al., 2011) showed that 30Hz stimulation gave better accuracy results and was also experienced as more comfortable by the subjects. As the template based classification uses one sequence period to construct a decision, faster bit stimulation results in shorter decision timing and also shorter training data collection. Both classifiers performed well with data from the best channel (O_Z), reaching >95% classification success in the best subjects. Combining information from different channels using a Bayesian fusion approach resulted in a decreased performance, showing that the key assumption that correlation scores for channels are conditionally independent is likely not true. A hierarchical Bayesian model incorporating higher order connectivity might give better performance. Training time was approximately 5 minutes in (Nezamfar, Orhan, Purwar et al., 2011) and 2.5 minutes in (Nezamfar, Orhan, Erdogmus et al., 2011).

Tagging with continuous Gaussian noise: ***Foxe et al. - Visually evoked spread spectrum response potential (VESPA)*** [2]
The visually evoked spread spectrum response potential (VESPA) method was described and then used extensively by the group at the Trinity College Institute of Neuroscience, Dublin, Ireland, headed by John J. Foxe. In contrast to the other BCI systems mentioned in this chapter that all use pseudorandom binary sequences, VESPA uses a Gaussian process to smoothly modulate the luminance of visual stimuli[3]. They justify this by annotating that m-sequences became popular due to their computational efficiency, but these days modern computers are sufficiently powerful that non-binary stimulus waveforms with arbitrary covariance structures can be generated and analysed. So instead of optimizing for computational convenience, focus should be on acquisition speed and unobtrusiveness.

The theoretical background of this technique is strongly overlapping with the auditory equivalent of this method, the AESPA, which was discussed in the previous chapter. Basic images such as a checkerboard pattern[4] are luminance modulated by an underlying spread spectrum waveform. This spread spectrum waveform is generated by amplitude-modifying a broadband noise carrier wave using Gaussian noise signals with normally distributed power over the range 0-30Hz. 30Hz is used as maximal value, as EEG power above 30Hz is usually very low. Waveforms with desired statistical properties are selected and stored. The spread spectrum waveform is mapped to the images according to a linear relation, with the zero point set to a certain luminance level (50%) or to a certain reference image, and scaled so that all stimuli scale approximately three standard deviations within the total displayable range.

EEG data is recorded using a 64 electrodes system filtered over the range 0-134Hz and digitized at a rate of 512Hz. Synchronization between stimulus delivery, stimulus luminance and EEG signal is encoded by including a signal from the parallel port of the presentation computer to the measured EEG signal. Signal pre-processing steps include digitally filtering of the EEG signal (offline) using a high-pass filter (pass band >2Hz, -60dB at 1Hz) and a low-pass filter (pass band <35Hz, -50dB at 45Hz), and calculation of the visual input signal by convolving the square wave commands given to the monitor with the monitor's response function.

The impulse response function of the visual system (referred as the VESPA) can be regarded as the superposition of all impulse responses, one per frame, each scaled by the associated input value. It is retrieved from the known stimulus waveform and the measured EEG signals by performing a linear least squares fit. The responses are measured using a sliding window starting 100 ms pre-stimulus to 400ms post-stimulus. (For a more in-depth description of the mathematics, see the appendix of (E. C. Lalor et al., 2006)). In 2008 a non-linear extension of the linear VESPA is presented, the quadratic VESPA, which includes both 1st-order and 2^{nd}-order values of the modulating system (E. C. Lalor, 2009; E. C. Lalor & Foxe, 2009). When this method was compared to the linear VESPA method the improvements found were very modest (E. C. Lalor, 2009).

In their first paper (E. C. Lalor et al., 2006) they present the VESPA method using snowflake shaped images, checkerboard patterns, and multiple simultaneous stimuli. Quantification of performance is obtained by comparing the method with the standard SSVEP, focussing on correlation values, reproducibility and signal-to-noise ratios. Both shapes elicit good results, with checkerboards giving stronger SNR and more reproducible VESPAs. Stimulation with multiple simultaneous stimuli gives multiple distinguishable VESPAs, with the fixated stimulus giving strongest results.

After introducing and showing the potential of their method (E. C. Lalor et al., 2006) and extending it with a quadratic VESPA (E. C. Lalor, 2009; E. C. Lalor & Foxe, 2009) and spatial frequency modulated stimuli (E. C. Lalor, Lucan, & Foxe, 2009), they use the method to investigate temporal frequency characteristics of the visual system (E. C. Lalor, Reilly, Pearlmutter, & Foxe, 2006), isolate endogenous visuo-spatial attentional effects (E. C. Lalor, Kelly, & Pearlmutter, 2007), early visual processing deficits in schizophrenia patients (E. C. Lalor, Yeap, Reilly, Pearlmutter, & Foxe, 2008), decoding velocities in the retina (E. C. Lalor, Ahmadian, & Paninski, 2009), magno- and parvocellular pathways (E. C. Lalor & Foxe, 2009) and early spatial attention modulation effects in the fovea (Frey, Kelly, Lalor, & Foxe, 2010).

Comparison of the different methods

Basic assumption

Both the pseudorandom sequence methods as the VESPA are based on the assumption that the EEG response to a stimulus is an attenuated, time-shifted version of simple components that the stimulus is considered to be composed of, and that the parameters of this impulse response can be recovered using a least-squares regression (E. C. Lalor et al., 2006; E. E. Sutter, 1992).

Modulation sequence

Most of the reviewed systems used a pseudorandom binary m-sequence whereas the VESPA method, like the AESPA method uses a Gaussian noise. In the discussion in chapter 5 the differences and implications will be discussed in more detail.

Stimulus shape

A number of different stimulus shapes have been tried successfully; the most recurring one was the checkerboard pattern. When compared with other stimuli, it was also reported as the most successful in eliciting responses, SNR and reproducibility (E. C. Lalor et al., 2006; E. E. Sutter, 1992). Colour alternations between red and green was found as a good alternative for luminance changes (flickering), as it was found to elicit responses almost as effective as flicker, while being much less tiring for the subjects (E. E. Sutter, 1992).

Estimating the impulse response function

A relatively simple basic template matching classifier was used in most of the studies, offering good results.
Classifiers are mainly used on the electrode with the best signal, but strong improvement of results was obtained using a multichannel identification method based on canonical correlation analysis (CCA) (Bin et al., 2011).
As the visual system does not behave as a purely linear system (E. E. Sutter, 1992), including the higher order values of the modulating system would be a logical step, however, either the gain was small (E. C. Lalor, 2009) or the classifier functioned worse than the basic version (Nezamfar, Orhan, Purwar et al., 2011).

Attentional effects

Strong attentional effects have been reported in almost all the studies that were mentioned. Due to retinal and cortical magnification, the focus of the gaze determines the majority of the elicit response. But also endogenous attention and motivation effects have a detrimental influence on the classification efficiency (E. C. Lalor et al., 2007). For instance Nezamfar removed one of the subjects from analysis, as the subject had reported that he had not been actively paying attention flickering checkerboards and had been occasionally visualizing other thoughts. His data analysis indeed showed only 40% accuracy, while other subjects performed normally (Nezamfar, Orhan, Purwar et al., 2011).

NOTES

[1] The use of temporal pseudorandom binary sequences to modify the luminance of a large field as a stimulus for clinical testing of visually evoked potentials (VEPs) was proposed prior to Sutters paper by (Srebro & Wright, 1980). In 1993 (Collins & Sawhney, 1993) used this pseudorandom binary sequence visual evoked response as a clinical tool for identifying lesions of the visual pathway.

[2] Unless noted otherwise, the information in the next six paragraphs is gathered from (E. C. Lalor et al., 2006).

[3] Although most of the papers using VESPA use luminance modulation, in (E. C. Lalor, Lucan et al., 2009) the feasibility of stochastic modulation of stimulus spatial frequency for eliciting VESPAs is shown.

[4] Basic images used as visual stimulus include:

- Snowflake images (E. C. Lalor et al., 2006)
- Checkerboards patterns (J. J. Foxe et al., 2008; E. C. Lalor et al., 2006; E. C. Lalor, 2009; E. C. Lalor, Lucan et al., 2009; E. C. Lalor et al., 2006; E. C. Lalor et al., 2007; E. C. Lalor & Foxe, 2009)
- Kanizsa illusory figures (E. C. Lalor et al., 2008)
- Rectangle blocks (Frey et al., 2010)
- Moving bars (E. C. Lalor et al., 2009)

CHAPTER 5 – DISCUSSION

In the previous chapters a number of different auditory and visual BCI systems were reviewed that make use of spread spectrum principles. Table 5.1 gives a global overview of all continuous and binary noise tagged VEP BCI systems discussed in this thesis. The systems' performances differed a lot; Mormose et al. got an information transfer rate of 10 bits/min., while the c-VEP system of Shangkai Gao's group managed to reach an average ITR of 108±12 bits/min. and a maximum ITR of 123 bits/min in one subject (Bin et al., 2011). This is on par with the fastest SSVEP-based BCI system at the moment, which reached a peak ITR of 124 bits/min., although average speeds of this BCI interface were significantly lower (ITR: 70±25 bit/min.) (Volosyak, 2011), showing the advantage of the use of spread codes in VEP-based BCI interfaces.

Most of the BCI systems examined in this thesis used one or multiple pseudorandom binary sequences, only the AESPA/VESPA uses Gaussian waveforms. Pseudorandom noise deviated from true Gaussian noise in several aspects. The second and higher order autocorrelates of Gaussian noise is zero, while those of (binary) PRN are substantially different (Swerup, 1978). The use of these PRN sequences as stimulus may therefor imply a certain degree of error when applied to non-linear systems.

Non-linearity and higher order analyses

Although most sensory-neural systems are generally non-linear, many non-linear systems can be described by a series of linear models. A complete description of a non-linear system includes the estimate of the first-order Wiener kernel, as well as the higher-order kernels, which can be obtained using random noise test signals (Marmarelis & Marmarelis, 1978). The estimation of the first-order Wiener kernel can be uncovered by cross-correlating the response of the system with the noise used as stimulus and then comparing the measured response with the response of a linear filter that has the obtained cross-correlogram as its impulse response (Møller & Angelo, 1988). As long as the higher-order auto-correlates of the noise used as stimulus are zero, the first order cross-correlation of the non-linear system is a valid estimate of the impulse response of the linear portion of that system (De Boer, 1976; Korenberg, 1973; Møller, 1986; Møller & Angelo, 1988; Swerup, 1978). The divergence between the modelled and the measured response contains the non-linear parts of the system, as well as other, uncorrelated, signals (Marmarelis & Marmarelis, 1978; Møller & Rees, 1986; Møller, 1986; Møller, 1987). These kinds of analyses, though potentially useful for understanding their performance and differences, were not used in the papers reviewed here.

Differences between systems – Gaussian noise vs. pseudorandom sequences

Use of binary PR sequences can thus be problematic when the sensory system contains strong higher-order non-linearities. Selecting the used pseudorandom noise codes on a low higher-level autocorrelation can help circumvent detection difficulties. Tertiary PR-sequences, not yet applied in BCI-systems, can be an option as well, as the even-order auto-correlates of tertiary PR-sequences are zero. However, the third-order autocorrelations suffer from anomalies (Godfrey, 1966; Gyftopoulos & Hooper, 1964; Møller & Angelo, 1988; Ream, 1970; Swerup, 1978), which affect the accuracy of the estimations of the first-order kernel when third- or higher-order non-linearities are present in the system (Møller, 1986; Møller & Angelo, 1988; Swerup, 1978).

Lalor et al. (2006) also suggest that Gaussian stimuli result in sharper estimated impulse responses which are more sensitive to changes in brain state and function (E. C. Lalor et al., 2006). They illustrate that using a simplified one-dimensional instantaneous stateless noise-free system (figure 5.1). A binary stimulus is only capable of eliciting extreme, saturated responses, as there are only two inputs (fig. 5a). This results in a slope of the response curve that is systematically lower that the slope of the response curve at the centre of its dynamic range. Non-saturating stimuli, such as Gaussian spread stimuli, are able to infer the whole input/output range (fig. 5b), giving a better approximation of the response curve.

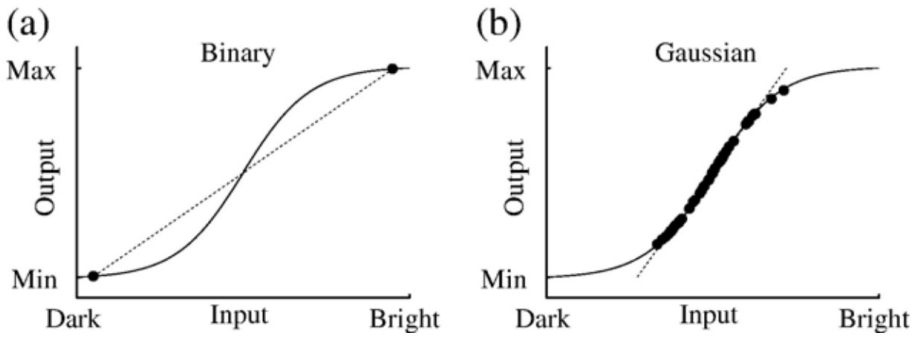

Figure 5.1: Simplified one-dimensional instantaneous stateless noise-free system.
The transfer function of a simplified one-dimensional instantaneous stateless noise-free system is represented by the sigmoid curves. When probing the system with a stimulus a corresponding output is measured (black dots). A) In the binary case only two possible inputs are available at the extremes. B) In the Gaussian input case also the non-extreme cases can be explored. The dashed line shows the linear approximation to the transfer function based on the samples.
[From: (E. C. Lalor et al., 2006) - figure 10]

Table 5.1: Overview of BCI-systems using spread spectrum stimuli.

A) Auditory BCI-systems				
BCI system (Group)	**Stimuli used** Image shapes / patterns	**Stimulus modulation**	**Major Findings**	**Information transfer rate** (average ITR)
AESPA (Foxe et al.)	- Broadband noise carrier wave - Pure tone carrier wave - Amplitude-envelope of natural speech	Amplitude modulation using Gaussian noise signals in the range of 0-30Hz	- Proved validity of approach as compared to standard AEP and for multiple simultaneously binaurally stimuli - Pure tone stimulus gave no significant results. - Correlation values and signal-to-noise ratios lower than AEP - Linear and quadratic modelling - Second and higher orders gave small improvements - Used in speech and (endo- and exogenous) attentional research	Not specified
Noise Tagging (Desain et al.)	Saw-tooth carrier wave	Amplitude modulation using binary Gold-sequences – 255 bits	- Proved validity of approach as compared with SSVEP - Training needed: 25 trials / 75 seconds - 91% classification rates using impulse-responses learned on one stimulus sequence	1.4 bits/min
B) Visual BCI-systems				
BCI system / group	**Stimuli used** Carrier wave / shapes	**Stimulus modulation**	**Major Findings**	**Information transfer rate** (average ITR)
Multifocal m-sequence technique (Sutter)	64 rectangular fields displayed as an 8x8 matrix with wrap around	Luminance modulation of targets using time-shifted versions of one m-sequence	- Prototype tested in 70 healthy and 20 disabled subjects. System applied in 1 ALS patient with intracranial EEG - Training lasting 10m up to 1h - Significant between-subject variations in optimal stimulation mode and rate - Colour alternation as effective as flickering targets, while being less tiring - check pattern reversals giving strongest performance - Patients often hindered by inadequate placement of electrodes and by EEG artefacts originating from involuntary muscle movement	10-12 words/minute (100>bits/min)
Eye gaze point detection (Momose et al.)	4 simultaneous presented characters (A, B, C and D)	Luminance modulation using 4 different m-sequences (9-bits)	- Subjects used gazing to select answer to simple questions. - Fundamental validity shown, but system insufficient for practical use - Training needed: 40.95s - Low concentration during target fixation and unstable kernel estimation increased the error rate	10 bits/min
c-VEP (Gao et al.)	16 // 32 rectangular fields displayed as an 4x4 // 4x8 matrix with wrap around	Luminance modulation of targets using time-shifted versions of one m-sequence (63-bits)	- Proved validity of approach as compared with SSVEP - Proved feasibility of method to measure interhemispheric transfer time - Training needed: 200 trials / 210 seconds - Single channel classification reaching >95% success in the best subjects - Multichannel identification method based on canonical correlation analysis (CCA) as target classifier	92.8±14.1 bits/min // 108±12 bits/min
Multiple c-VEP (Nezamfar et al.)	Two inverted 10x10 checkerboard patterns	Inverting of pattern determined by 4 different m-sequences (31-bits), modulation rate 15 or 30Hz	- Proved validity of approach as compared with SSVEP - Training needed: 2.5 min // 5 min - 30Hz stimulation gave better accuracy results and was experienced as more comfortable - Multichannel identification method based on Bayesian fusion approach did not improved target identification	Not specified
VESPA (Foxe et al.)	- Checkerboard patterns - Kanizsa illusory figures - Moving bars - Rectangle blocks - Snowflake images	Luminance modulation and/or spatial modulation using Gaussian noise signals in the range of 0-30Hz	- Proved validity of approach as compared to standard AEP and for multiple simultaneously stimuli (overlapping and non-overlapping) - Linear and quadratic modelling - Second and higher orders gave small improvements - Used to investigate temporal frequency characteristics, endogenous and early spatial attentional modulation, retina velocities, magno- and parvocellular pathways and visual processing deficits in schizophrenia.	Not specified

The drawback of using Gaussian noise signals is their mathematical complexity and computational load. With current computer performance this is becoming less of a limitation than it used to be up to a few years ago. As the stimuli used in a BCI-system can be constructed beforehand (off-line), it is possible to calculate pure Gaussian waveforms with good characteristics, as is applied in AESPA and VESPA (E. C. Lalor et al., 2006; A. J. Power et al., 2007). The auteurs do not elaborate how they select their preferred waveforms.

Differences between systems – Stimuli delivery

The methods discussed have used a number of different stimulus-shapes to be modulated or tagged by noise. A noteworthy difference between the auditory and visual techniques is that with visual stimulation the spread spectrum sequence itself can be directly used as a stimulus, for instance by using it to control the flashing of a light or pattern, while the auditory stimulus setup forces the use of a carrier waveform. AESPA shows that for the carrier signal a broadband noise waveform can be used here, resulting in a completely spread stimulus (A. J. Power et al., 2007). However, when presenting more stimuli simultaneously in an attention-based paradigm, it might be more useful to amplitude-modulate a more recognizable sequence, such as a saw-tone (Farquhar et al., 2008), natural speech (A. J. Power et al., 2012) or a fragment of music, as these stimuli are easier to recognize and thus making it easier for the subject to attend to one of them. Also, modulated music or speech may give a higher comfort level for the user than seemingly random hiss, especially when the system has to be used for long durations. Note that the emotional load attached to such carriers is known to affect the strength of event-related potentials (Molina, Tsoneva, & Nijholt, 2009) and VEPs (Kemp, Gray, Silberstein, Armstrong, & Nathan, 2004).

In visual systems modulation of a checkerboard pattern reversal gives the strongest results (E. C. Lalor et al., 2006; E. E. Sutter, 1992). Flickering stimuli provide the best responses, with more pronounced differences between stimuli states giving stronger responses, but these provide less comfort for the user (Bieger & Molina, 2010). Colour alternations are described by subjects as less tiring, while performing almost as effective as flicker (E. E. Sutter, 1992). Superimposing pictures on a modulated background may help rise comfort levels, as it is more pleasant to look at meaningful pictures than only to a flashing checkerboard pattern, but as with the music-stimuli, emotional value of the image may influence the strength of the responses.

When multiple stimuli are presented simultaneously, a matrix presentation with wrap-around can help in ensuring the equivalence of the target stimuli responses (figure 4.1) (Bin et al., 2011; E. E. Sutter, 1992). In a visual BCI-system targeting of a specific stimulus can be accomplished by gaze-shifting or selective attention modulation. The stimulus captured in the central visual field generates much stronger brain responses than those in the periphery of the visual field (E. E. Sutter, 1992; E. Sutter, 1985) and an attended stimulus generates a stronger response than an unattended stimulus (E. C. Lalor et al., 2006). Most methods described here that employ multiple stimuli simultaneous actually use a combination of these two target enhancement methods. For severely disabled patients reliable gaze control might not be an option, in which case overlapping stimuli might be employed (Zhu, Bieger, Molina, & Aarts, 2010). This strategy has been employed in a number of SSVEP-BCI systems (Allison et al., 2008; Y. Chen, Seth, Gally, & Edelman, 2003; Cheng, Gao, Gao, & Xu, 2001). With VESPA a successful trial using overlapping stimuli of unequal size was performed (E. C. Lalor et al., 2006), though some spatial discrepancy between the two stimuli could induce gaze-shifting effects, making the targeting in this trial not purely attention based.

The maximum number of simultaneous presented stimuli has a strong impact on the information transfer rate of the system, especially in a P300 -speller-like setup, as it directly determines the number of key functions the subject can pick from. Due to their low anti-interference and multi-user properties, spread spectrum signals offer a much wider range of possible stimuli than steady stated evoked potentials, as there the number of non-overlapping frequencies that elicit equivalent responses is limited. M-sequences offer good auto-correlation properties, but cross-correlation of two m-sequences tends to be large, so only the subset of 'preferred pair' m-sequences with predictable and optimal (low) cross-correlation properties are eligible (Delgado & Ozdamar, 2004; Niho, 1972; Sarwate & Pursley, 1980; Tirkel, 1996). Although the auto-correlation functions of Gold and Kasami codes are less optimal as compared to m-sequences (Gold, 1967; Kasami, 1966), the large sets of equal-length sequences with controlled cross-correlation properties they provide makes them more suitable in a multiple stimuli environment, with Gold codes offering better performance than Kasami codes (Turkmani & Goni, 1993).

Differences between systems – Testing in healthy subjects vs. patients

Except for Sutter (1992), all systems discussed here were only tested on healthy subjects. Granting this is not that unusual considering the early stages of this method in a BCI-context, this may entail some difficulties. Sutter noted hindrances when his system was applied for an extensive time, of which some were specific for disabled persons. It would therefore be desirable to have more of these systems tested not only on healthy participants, but also on (disabled) patients, who form a substantial fraction of the target audience of these kinds of systems.

Further reading

For this thesis the technical details were kept to a moderate level, so the information is palatable for laymen from related and unrelated disciplines. For a deeper theoretical and technical insight the following papers are recommended:

- For a deeper insight in the (higher order) kernel characteristics of pseudorandom VEPs:

(Nemoto, Momose, Kiyosawa, Mori, & Mochizuki, 2004; E. E. Sutter, 2001)

- Determination of temporal frequency characteristic (TFC) of the visual system obtained using pseudorandomly elicit VEPs:
(K. Momose et al., 1999)

- Deconvolution of overlapping evoked potentials:
(Bohórquez & Özdamar, 2006; Delgado & Ozdamar, 2004; Desain et al., 2008)

Conclusion

Spread spectrum elicited VEPs offer a valuable extension of the palette of VEPs available for BCI-systems. Their favourable auto- and cross-correlation characteristics provide good anti-interference properties, which make them especially beneficial in systems using multiple simultaneously presented stimuli, like speller-setups. The high performances reached by some of these systems prove the viability of this cutting edge technique, and for the (near) future an increase of papers on BCI systems is anticipated. And next to their application in practical BCI's, these signals are promising as a new kind of probe for the scientific inquiry into the operation of perceptual and attentional systems.

REFERENCES

Agus, T. R., Thorpe, S. J., & Pressnitzer, D. (2010). Rapid formation of robust auditory memories: insights from noise. *Neuron, 66*(4), 610-618.

Al-Bassam, S., & Bose, B. (1990). On balanced codes. *Information Theory, IEEE Transactions on, 36*(2), 406-408.

Allison, B. Z., McFarland, D. J., Schalk, G., Zheng, S. D., Jackson, M. M., & Wolpaw, J. R. (2008). Towards an independent brain-computer interface using steady state visual evoked potentials. *Clinical Neurophysiology, 119*(2), 399-408.

Bahramisharif, A., Van Gerven, M., Heskes, T., & Jensen, O. (2010). Covert attention allows for continuous control of brain–computer interfaces. *European Journal of Neuroscience, 31*(8), 1501-1508.

Bar-David, I., & Krishnamoorthy, R. (1996). Barker code position modulation for high-rate communication in the ISM bands. *Bell Labs Technical Journal, 1*(2), 21-40.

Barker, R. (1953). Group synchronizing of binary digital systems. *Communication Theory, ,* 273-287.

Benedetto, S., & Montorsi, G. (1996). Serial concatenation of block and convolutional codes. *Electronics Letters, 32*(10), 887-888.

Berrou, C., Glavieux, A., & Thitimajshima, P. (1993). Near Shannon limit error-correcting coding and decoding: Turbo-codes. 1. Paper presented at the *Communications, 1993. ICC 93. Geneva. Technical Program, Conference Record, IEEE International Conference on, , 2* 1064-1070 vol. 2.

Biao Zhang, Jianjun Wang, & Fuhlbrigge, T. (2010). A review of the commercial brain-computer interface technology from perspective of industrial robotics. Paper presented at the *Automation and Logistics (ICAL), 2010 IEEE International Conference on,* 379-384.

Bieger, J., & Molina, G. (2010). *Light Stimulation Properties to Influence Brain Activity: A Brain-Computer Interface Application,*

Bin, G., Gao, X., Wang, Y., Hong, B., & Gao, S. (2009). VEP-based brain-computer interfaces: time, frequency, and code modulations. *Computational Intelligence Magazine, IEEE, 4*(4), 22-26.

Bin, G., Gao, X., Wang, Y., Li, Y., Hong, B., & Gao, S. (2011). A high-speed BCI based on code modulation VEP. *Journal of Neural Engineering, 8*, 025015.

Birbaumer, N., Ghanayim, N., Hinterberger, T., Iversen, I., Kotchoubey, B., Kubler, A., . . . Flor, H. (1999). A spelling device for the paralysed. *Nature, 398*(6725), 297-298.

Birbaumer, N., Elbert, T., Canavan, A., & Rockstroh, B. (1990). Slow potentials of the cerebral cortex and behavior. *Physiol Rev, 70*(1), 1-41.

Birbaumer, N., & Cohen, L. G. (2007). Brain computer interfaces: communication and restoration of movement in paralysis. *The Journal of Physiology, 579*(3), 621-636. doi:10.1113/jphysiol.2006.125633

Blankertz, B., Tangermann, M., Vidaurre, C., Fazli, S., Sannelli, C., Haufe, S., . . . Muller, K. R. (2010). The Berlin Brain-Computer Interface: Non-Medical Uses of BCI Technology. *Frontiers in Neuroscience, 4*, 198.

Blankespoor, J. (2008). Noise Tagging as a New Auditory BCI-Paradigm: a Pilot Study. *Master Thesis, Radboud University, Nijmegen. Available at http://www.nici.ru.nl/mmm/papers/JoelleBlankespoor.pdf*

Bohórquez, J., & Özdamar, Ö. (2006). Signal to noise ratio analysis of maximum length sequence deconvolution of overlapping evoked potentials. *The Journal of the Acoustical Society of America, 119*, 2881.

Borwein, P., & Mossinghoff, M. (2008). Barker sequences and flat polynomials. *London Mathematical Society Lecture note series, 352*, 71.

Breitwieser, C., Pokorny, C., Neuper, C., & Muller-Putz, G. R. (2011). Somatosensory evoked potentials elicited by stimulating two fingers from one hand — Usable for BCI?, Paper presented at the *Engineering in Medicine and Biology Society,EMBC, 2011 Annual International Conference of the IEEE,* 6373-6376.

Buehrer, R. M. (2006). Code division multiple access (CDMA). *Synthesis Lectures on Communications, 1*(1), 1-192.

Buracas, G. T., & Boynton, G. M. (2002). Efficient design of event-related fMRI experiments using M-sequences. *NeuroImage, 16*(3), 801-813.

Chen, Y., Seth, A. K., Gally, J. A., & Edelman, G. M. (2003). The power of human brain magnetoencephalographic signals can be modulated up or down by changes in an attentive visual task. *Proceedings of the National Academy of Sciences, 100*(6), 3501.

Chen, Z., Hu, G., Glasberg, B. R., & Moore, B. C. J. (2011). A new method of calculating auditory excitation patterns and loudness for steady sounds. *Hearing Research,*

Cheng, M., Gao, X., Gao, S., & Xu, D. (2001). Multiple color stimulus induced steady state visual evoked potentials. Paper presented at the *Engineering in Medicine and Biology Society, 2001. Proceedings of the 23rd Annual International Conference of the IEEE, , 2* 1012-1014 vol. 2.

Christopher deCharms, R. (2008). Applications of real-time fMRI. *Nature Reviews. Neuroscience, 9*(9), 720-729.

Chung, S. Y., Forney Jr, G. D., Richardson, T. J., & Urbanke, R. (2001). On the design of low-density parity-check codes within 0.0045 dB of the Shannon limit. *Communications Letters, IEEE, 5*(2), 58-60.

Chung, S. Y., Richardson, T. J., & Urbanke, R. L. (2001). Analysis of sum-product decoding of low-density parity-check codes using a Gaussian approximation. *Information Theory, IEEE Transactions on, 47*(2), 657-670.

Collins, A. D., & Sawhney, B. B. (1993). Pseudorandom binary sequence stimulation applied to the visual evoked response. *Documenta Ophthalmologica, 83*(2), 163-173.

Cook, C., & Marsh, H. (1983). An introduction to spread spectrum. *IEEE Communications Magazine, 21*(2), 8-16.

Cuddlyable3 at en.wikipedia. (2008). *16-bit Fibonacci LFSR SIG* [LFSR-F16.gif, Original uploader was Cuddlyable3 at en.wikipedia, Released into the public domain (by the author), Downloaded 2/26/2012 from https://commons.wikimedia.org/wiki/File:LFSR-F16.gif] (14 June 2008 ed.)

D Terr, E. W. (2012). *"Barker Code" from MathWorld - A Wolfram Web Resource.* Retrieved 4/30, 2012, from http://mathworld.wolfram.com/BarkerCode.html

De Boer, E. (1976). Cross-correlation function of a bandpass nonlinear network. *Proceedings of the IEEE, 64*(9), 1443-1444.

Delgado, R. E., & Ozdamar, O. (2004). Deconvolution of evoked responses obtained at high stimulus rates. *The Journal of the Acoustical Society of America, 115*, 1242.

Desain, P., Farquhar, J., Blankespoor, J., & Gielen, S. (2008). Detecting spread spectrum pseudo random noise tags in EEG/MEG using a structure-based decomposition. Paper presented at the *4th Int. BCI Workshop and Training Course.*

Dinan, E. H., & Jabbari, B. (1998). Spreading codes for direct sequence CDMA and wideband CDMA cellular networks. *Communications Magazine, IEEE, 36*(9), 48-54.

Divsalar, D., Jin, H., & McEliece, R. J. (1998). Coding theorems for" turbo-like" codes. Paper presented at the *Proceedings Of The Annual Allerton Conference On Communication Control And Computing, 36* 201-210.

Drullman, R., Festen, J. M., & Plomp, R. (1994a). Effect of reducing slow temporal modulations on speech reception. *The Journal of the Acoustical Society of America, 95*, 2670.

Drullman, R., Festen, J. M., & Plomp, R. (1994b). Effect of temporal envelope smearing on speech reception. *The Journal of the Acoustical Society of America, 95*, 1053.

Farquhar, J., Blankespoor, J., Vlek, R., & Desain, P. (2008). Towards a noise-tagging auditory BCI-paradigm. Paper presented at the *Proceedings of the 4th International Brain-Computer Interface Workshop and Training Course,* 50-55.

Farwell, L. A., & Donchin, E. (1988). Talking off the top of your head: toward a mental prosthesis utilizing event-related brain potentials. *Electroencephalography and Clinical Neurophysiology, 70*(6), 510-523. doi:10.1016/0013-4694(88)90149-6

Fossorier, M. P. C. (2004). Quasicyclic low-density parity-check codes from circulant permutation matrices. *Information Theory, IEEE Transactions on, 50*(8), 1788-1793.

Foxe, J. J., Strugstad, E. C., Sehatpour, P., Molholm, S., Pasieka, W., Schroeder, C. E., & McCourt, M. E. (2008). Parvocellular and magnocellular contributions to the initial generators of the visual evoked potential: high-density electrical mapping of the "C1" component. *Brain Topography, 21*(1), 11-21.

Foxe, J., Lalor, E., Power, A., & Reilly, R. (2009). Resolving Precise Temporal Processing Properties of the Auditory System Using Continuous Stimuli. *Journal of Neurophysiology, 102*(1), 349-359.

Frey, H. P., Kelly, S. P., Lalor, E. C., & Foxe, J. J. (2010). Early spatial attentional modulation of inputs to the fovea. *The Journal of Neuroscience, 30*(13), 4547-4551.

Gallager, R. (1962). Low-density parity-check codes. *Information Theory, IRE Transactions on, 8*(1), 21-28.

Gerven, M., Farquhar, J., Schaefer, R., Vlek, R., Geuze, J., Nijholt, A., . . . Gielen, S. (2009). The brain–computer interface cycle. *Journal of Neural Engineering, 6*, 041001.

Godfrey, K. (1966). Three-level m sequences. *Electronics Letters, 2*(7), 241-243.

Gold, R. (1967). Optimal binary sequences for spread spectrum multiplexing (Corresp.). *Information Theory, IEEE Transactions on, 13*(4), 619-621.

Golomb, S. W., Welch, L. R., Goldstein, R. M., & Hales, A. W. (1967). *Shift register sequences* Holden-Day San Francisco.

Green, D. M. (1988). *Profile analysis: Auditory intensity discrimination* Oxford University Press, USA.

Gürkök, H., & Nijholt, A. (2011). Brain-computer interfaces for multimodal interaction: a survey and principles.

Guttman, N., & Julesz, B. (1963). Lower limits of auditory periodicity analysis. *The Journal of the Acoustical Society of America, 35*, 610.

Gyftopoulos, E. P., & Hooper, R. J. (1964). *Signals for Transfer Function Measurements in Nonlinear Systems,*

Hamadicharef, B., Haihong Zhang, Cuntai Guan, Chuanchu Wang, Kok Soon Phua, Keng Peng Tee, & Kai Keng Ang. (2009). Learning EEG-based spectral-spatial patterns for attention level measurement. Paper presented at the *Circuits and Systems, 2009. ISCAS 2009. IEEE International Symposium on,* 1465-1468.

Hammond, J., & Purington, E. (1957). A History of Some Foundations of Modern Radio-Electronic Technology. *Proceedings of the IRE, 45*(9), 1191-1208.

Haselager, P., Vlek, R., Hill, J., & Nijboer, F. (2009). A note on ethical aspects of BCI. *Neural Networks, 22*(9), 1352-1357.

Hill, J., Farquhar, J., Martens, S., Bießmann, F., & Schölkopf, B. (2009). Effects of stimulus type and of error-correcting code design on BCI speller performance.

Hillyard, S. A., Hink, R. F., Schwent, V. L., & Picton, T. W. (1973). Electrical signs of selective attention in the human brain. *Science, 182*(4108), 177-180.

Hinterberger, T., Schmidt, S., Neumann, N., Mellinger, J., Blankertz, B., Curio, G., & Birbaumer, N. (2004). Brain-computer communication and slow cortical potentials. *IEEE Trans Biomed Eng, 51*(6), 1011-1018.

Hochberg, L. R., Serruya, M. D., Friehs, G. M., Mukand, J. A., Saleh, M., Caplan, A. H., . . . Donoghue, J. P. (2006). Neuronal ensemble control of prosthetic devices by a human with tetraplegia. *Nature, 442*(7099), 164-171.

Holmes, J. K. (2007). *Spread spectrum systems for GNSS and wireless communications* Artech House.

Hou, J., Siegel, P. H., & Milstein, L. B. (2001). Performance analysis and code optimization of low density parity-check codes on Rayleigh fading channels. *Selected Areas in Communications, IEEE Journal on, 19*(5), 924-934.

Huggins, J. E., Wren, P. A., & Gruis, K. L. (2011). What would brain-computer interface users want? Opinions and priorities of potential users with amyotrophic lateral sclerosis. *Amyotrophic Lateral Sclerosis,* (0), 1-8.

Ikeda, S., Tanaka, T., & Amari, S. (2004). Information geometry of turbo and low-density parity-check codes. *Information Theory, IEEE Transactions on, 50*(6), 1097-1114.

Jia, X., Smith, M. A., & Kohn, A. (2011). Stimulus selectivity and spatial coherence of gamma components of the local field potential. *The Journal of Neuroscience, 31*(25), 9390-9403.

Jin, H., Khandekar, A., & McEliece, R. (2000). Irregular repeat-accumulate codes. Paper presented at the *Proc. 2nd Int. Symp. Turbo Codes and Related Topics,* 1-8.

Julesz, B., & Guttman, N. (1963). Auditory memory. *The Journal of the Acoustical Society of America, 35*, 1895.

Kasami, T. (1966). Weight distribution formula for some class of cyclic codes.

Katzner, S., Nauhaus, I., Benucci, A., Bonin, V., Ringach, D. L., & Carandini, M. (2009). Local origin of field potentials in visual cortex. *Neuron, 61*(1), 35-41.

Kemp, A. H., Gray, M. A., Silberstein, R. B., Armstrong, S. M., & Nathan, P. J. (2004). Augmentation of serotonin enhances pleasant and suppresses unpleasant cortical electrophysiological responses to visual emotional stimuli in humans. *NeuroImage, 22*(3), 1084-1096.

Knuth, D. (1986). Efficient balanced codes. *Information Theory, IEEE Transactions on, 32*(1), 51-53.

Korenberg, M. (1973). Cross-correlation analysis of neural cascades. Paper presented at the *Proc. 10th Ann. Rocky Mountain Bioeng. Symp, , 1* 47-52.

Kronegg, J., Voloshynovskiy, S., & Pun, T. (2005). Analysis of bit-rate definitions for brain-computer interfaces. Paper presented at the *Int. Conf. on Human-Computer Interaction (HCI'05), Las Vegas, Nevada, USA, , 12* 18.

Kübler, A., Nijboer, F., Mellinger, J., Vaughan, T. M., Pawelzik, H., Schalk, G., . . . Wolpaw, J. R. (2005). Patients with ALS can use sensorimotor rhythms to operate a brain-computer interface. *Neurology, 64*(10), 1775-1777.

Lacey, S., Stilla, R., & Sathian, K. (2012). Metaphorically feeling: Comprehending textural metaphors activates somatosensory cortex. *Brain and Language.*

Lai, T. Y. Y., Chan, W. M., Lai, R. Y. K., Ngai, J. W. S., Li, H., & Lam, D. S. C. (2007). The clinical applications of multifocal electroretinography: a systematic review. *Survey of Ophthalmology, 52*(1), 61-96.

Lalor, E. C. (2009). Modeling the human visual system using the white-noise approach. Paper presented at the *Neural Engineering, 2009. NER'09. 4th International IEEE/EMBS Conference on,* 589-592.

Lalor, E. C., Ahmadian, Y., & Paninski, L. (2009). The relationship between optimal and biologically plausible decoding of stimulus velocity in the retina. *JOSA A, 26*(11), B25-B42.

Lalor, E. C., Lucan, J. N., & Foxe, J. J. (2009). Estimation of the impulse response of the visual system using stochastic modulation of stimulus spatial frequency. Paper presented at the *Neural Engineering, 2009. NER'09. 4th International IEEE/EMBS Conference on,* 593-596.

Lalor, E. C., Reilly, R. B., Pearlmutter, B. A., & Foxe, J. J. (2006). A spectrum of colors: investigating the temporal frequency characteristics of the human visual system using a system identification approach. Paper presented at the *Engineering in Medicine and Biology Society, 2006. EMBS'06. 28th Annual International Conference of the IEEE,* 3720-3723.

Lalor, E. C., & Foxe, J. J. (2009). Visual evoked spread spectrum analysis (VESPA) responses to stimuli biased towards magnocellular and parvocellular pathways. *Vision Research, 49*(1), 127-133.

Lalor, E. C., & Foxe, J. J. (2010). Neural responses to uninterrupted natural speech can be extracted with precise temporal resolution. *European Journal of Neuroscience, 31*(1), p189-5p.

Lalor, E. C., Kelly, S. P., & Pearlmutter, B. A. (2007). Isolating endogenous visuo-spatial attentional effects using the novel visual-evoked spread spectrum analysis (VESPA) technique. *European Journal of Neuroscience, 26*(12), p3536-7p.

Lalor, E. C., Pearlmutter, B. A., Reilly, R. B., McDarby, G., & Foxe, J. J. (2006). The VESPA: A method for the rapid estimation of a visual evoked potential. *NeuroImage, 32*(4), 1549-1561.

Lalor, E. C., Yeap, S., Reilly, R. B., Pearlmutter, B. A., & Foxe, J. J. (2008). Dissecting the cellular contributions to early visual sensory processing deficits in schizophrenia using the VESPA evoked response. *Schizophrenia Research, 98*(1-3), 256-264.

Langton, C. (2002). *Tutorial 25 - Spread spectrum and CDMA.* (Tutorial). *Available on http://www.complextoreal.com/CDMA.pdf*

Le Goff, S., Glavieux, A., & Berrou, C. (1994). Turbo-codes and high spectral efficiency modulation. Paper presented at the *Communications, 1994. ICC'94, SUPERCOMM/ICC'94, Conference Record,'Serving Humanity through Communications.'IEEE International Conference on,* 645-649 vol. 2.

Leiner, B. M. J. (2005). LDPC Codes–a brief Tutorial. *Stud.ID.: 53418L April, 8*, 8.

Leins, U., Goth, G., Hinterberger, T., Klinger, C., Rumpf, N., & Strehl, U. (2007). *Neurofeedback for Children with ADHD: A Comparison of SCP and Theta/Beta Protocols* Springer Netherlands. doi:10.1007/s10484-007-9031-0

Li, Z., Chen, L., Zeng, L., Lin, S., & Fong, W. H. (2006). Efficient encoding of quasi-cyclic low-density parity-check codes. *Communications, IEEE Transactions on, 54*(1), 71-81.

Li, Y., Bin, G., Hong, B., & Gao, X. (2010). A coded VEP method to measure interhemispheric transfer time (IHTT). *Neuroscience Letters, 472*(2), 123-127.

Longstreet, D. L. (2008). *Spread Spectrum Communication Turorial with an Example in CDMA.* (No. EET 411 Communication Systems).

Luby, M. G., Mitzenmacher, M., Shokrollahi, M. A., & Spielman, D. A. (2001). Improved low-density parity-check codes using irregular graphs. *Information Theory, IEEE Transactions on, 47*(2), 585-598.

Marmarelis, P. Z., & Marmarelis, V. Z. (1978). *Analysis of physiological systems: The white-noise approach* Plenum Press New York.

Martens, S., Hill, N., Farquhar, J., & Schölkopf, B. (2007). Impact of target-to-target interval on classification performance in the P300 speller. Paper presented at the *Applied Neuroscience Conference,*

Martens, S., Hill, N., Farquhar, J., & Schölkopf, B. (2009). Overlap and refractory effects in a brain–computer interface speller based on the visual P300 event-related potential. *Journal of Neural Engineering, 6*, 026003.

Maye, A., Zhang, D., Wang, Y., Gao, S., & Engel, A. K. (2011). Multimodal Brain-Computer Interfaces. *Tsinghua Science & Technology, 16*(2), 133-139.

Meel, J. (1999). Spread Spectrum: Introduction. *Spread Spectrum Scene,*

Middendorf, M., McMillan, G., Calhoun, G., & Jones, K. S. (2000). Brain-computer interfaces based on the steady-state visual-evoked response. *IEEE Transactions on Rehabilitation Engineering : A Publication of the IEEE Engineering in Medicine and Biology Society, 8*(2), 211-214.

Mitra, A. (2007). On pseudo-random and orthogonal binary spreading sequences. *Int.J.Info.Tech, 4*(2), 137-144.

Molina, G. G., Tsoneva, T., & Nijholt, A. (2009). Emotional brain-computer interfaces. Paper presented at the *Affective Computing and Intelligent Interaction and Workshops, 2009. ACII 2009. 3rd International Conference on,* 1-9.

Møller, A. R. (1977). Frequency selectivity of single auditory-nerve fibers in response to broadband noise stimuli. *The Journal of the Acoustical Society of America, 62*, 135.

Møller, A. R. (1986). Systems identification using pseudorandom noise applied to a sensorineural system. *Computers & Mathematics with Applications, 12*(6), 803-814.

Møller, A. R. (1987). Auditory evoked potentials to continuous amplitude-modulated sounds: can they be described by linear models? *Electroencephalography and Clinical Neurophysiology, 66*(1), 56-65.

Møller, A. R., & Angelo, R. M. (1988). Use of pseudorandom noise in studies of auditory evoked potentials. *Annals of Biomedical Engineering, 16*(1), 35-51.

Møller, A. R., & Jannetta, P. J. (1983). Interpretation of brainstem auditory evoked potentials: results from intracranial recordings in humans. *Scandinavian Audiology, 12*(2), 125-133.

Møller, A. R., & Jho, H. D. (1989). Responses from the exposed human auditory nerve to pseudorandom noise. *Hearing Research, 42*(2-3), 237-252.

Møller, A. R., & Rees, A. (1986). Dynamic properties of the responses of single neurons in the inferior colliculus of the rat. *Hearing Research, 24*(3), 203-215.

Momose, K., Kiyosawa, M., Nemoto, N., Kimura, Y., Okuyama, F., & Senda, M. (1999). Visual temporal frequency characteristics determined by pseudorandom stimuli. *Investigative Ophthalmology & Visual Science, 40*(1), 50-54.

Momose, K. (2007). Evaluation of an eye gaze point detection method using VEP elicited by multi-pseudorandom stimulation for brain computer interface. Paper presented at the *Engineering in Medicine and Biology Society, 2007. EMBS 2007. 29th Annual International Conference of the IEEE,* 5063-5066.

Muller-Putz, G., Scherer, R., Neuper, C., & Pfurtscheller, G. (2006). Steady-state somatosensory evoked potentials: suitable brain signals for brain-computer interfaces? *IEEE Trans Neural Syst Rehabil Eng, 14*(1), 30-37.

Nemoto, N., Momose, K., Kiyosawa, M., Mori, H., & Mochizuki, M. (2004). Characteristics of first and second order kernels of visually evoked potentials elicited by pseudorandom stimulation. *Documenta Ophthalmologica, 108*(2), 157-163.

Nezamfar, H., Orhan, U., Erdogmus, D., Hild, K., Purwar, S., Oken, B., & Fried-Oken, M. (2011). On visually evoked potentials in eeg induced by multiple pseudorandom binary sequences for brain computer interface design. Paper presented at the *Acoustics, Speech and Signal Processing (ICASSP), 2011 IEEE International Conference on,* 2044-2047.

Nezamfar, H., Orhan, U., Purwar, S., Hild, K., Oken, B., & Erdogmus, D. (2011). Decoding of multichannel EEG activity from the visual cortex in response to pseudorandom binary sequences of visual stimuli. *International Journal of Imaging Systems and Technology, 21*(2), 139-147.

Nicolas-Alonso, L. F., & Gomez-Gil, J. (2012). Brain Computer Interfaces, a Review. *Sensors, 12*(2), 1211-1279.

Nicolelis, M. A. L. (2003). Brain-machine interfaces to restore motor function and probe neural circuits. *Nature Reviews. Neuroscience, 4*(5), 417-422.

Niho, Y. (1972). *Multi-Valued Cross-Correlation Functions between Two Maximal Linear Recursive Sequences.,*

Nijboer, F., Clausen, J., Allison, B. Z., & Haselager, P. (2011a). The Asilomar Survey: Stakeholders' Opinions on Ethical Issues Related to Brain-Computer Interfacing. *Neuroethics,* , 1-38.

Nijboer, F., Clausen, J., Allison, B., & Haselager, P. (2011b). Researchers' opinions about ethically sound dissemination of BCI research to the public media. *International Journal of Bioelectromagnetism, 13*(3), 108-109.

Nijboer, F., Matuz, T., Kübler, A., & Birbaumer, N. (2006). Ethical, psychological and social implications of brain-computer interface application in paralyzed patients. *Bioethics,* , 48-50.

Nijholt, A., & Tan, D. (2008). Brain-Computer Interfacing for Intelligent Systems. *Intelligent Systems, IEEE, 23*(3), 72-79.

Nijholt, A., Allison, B. Z., & Jacob, R. J. K. (2011). *Brain-computer interaction: can multimodality help?* Alicante, Spain: ACM.

Nijholt, A., Bos, D. P., & Reuderink, B. (2009). Turning shortcomings into challenges: Brain–computer interfaces for games. *Entertainment Computing, 1*(2), 85-94. doi:10.1016/j.entcom.2009.09.007

Nijholt, A., Tan, D., Allison, B., Milan, J. d. R., & Graimann, B. (2008). *Brain-computer interfaces for hci and games*. Florence, Italy: ACM.

Oksman, V., & Galli, S. (2009). G. hn: The new ITU-T home networking standard. *Communications Magazine, IEEE, 47*(10), 138-145.

O'Leary, D., & Honrubia, V. (1975). On-line identification of sensory systems using pseudorandom binary noise perturbations. *Biophysical Journal, 15*(6), 505-532.

Ortner, R., Allison, B. Z., Korisek, G., Gaggl, H., & Pfurtscheller, G. (2011). An SSVEP BCI to Control a Hand Orthosis for Persons With Tetraplegia. *Neural Systems and Rehabilitation Engineering, IEEE Transactions on, 19*(1), 1-5.

Parks, S., Keating, D., & Evans, A. (2002). The Wide Field Multifocal ERG: A Review of 2151 Investigations. *ARVO Meeting Abstracts, 43*(12), 1794.

Pasqualotto, E., Federici, S., & Belardinelli, M. O. (2012). Toward functioning and usable brain-computer interfaces (BCIs): a literature review. *Disability and Rehabilitation.Assistive Technology, 7*(2), 89-103. doi:10.3109/17483107.2011.589486; 10.3109/17483107.2011.589486

Pfurtscheller, G., & Lopes da Silva, F. H. (1999). Event-related EEG/MEG synchronization and desynchronization: basic principles. *Clinical Neurophysiology, 110*(11), 1842-1857. doi:10.1016/S1388-2457(99)00141-8

Pickholtz, R., Schilling, D., & Milstein, L. (1982). Theory of Spread-Spectrum Communications - A Tutorial. *Communications, IEEE Transactions on, 30*(5), 855-884.

Plass-Oude Bos, D., Reuderink, B., Laar, B., Gürkök, H., Mühl, C., Poel, M., . . . Heylen, D. (2010). Brain-computer interfacing and games. *Brain-Computer Interfaces, *, 149-178.

Plourde, G. (2006). Auditory evoked potentials. *Best Practice & Research Clinical Anaesthesiology, 20*(1), 129-139.

Power, A. J., Foxe, J. J., Forde, E. J., Reilly, R. B., & Lalor, E. C. (2012). At what time is the cocktail party? A late locus of selective attention to natural speech. *European Journal of Neuroscience,*

Power, A. J., Lalor, E. C., & Reilly, R. B. (2007). Eliciting audio evoked potentials using continuous stimuli. Paper presented at the *Engineering in Medicine and Biology Society, 2007. EMBS 2007. 29th Annual International Conference of the IEEE,* 4264-4267.

Power, A. J., Lalor, E. C., & Reilly, R. B. (2009). Extracting separate responses to simultaneously presented continuous auditory stimuli: An auditory attention study. Paper presented at the *Neural Engineering, 2009. NER'09. 4th International IEEE/EMBS Conference on,* 502-505.

Power, A. J., Lalor, E. C., & Reilly, R. B. (2011). Endogenous auditory spatial attention modulates obligatory sensory activity in auditory cortex. *Cerebral Cortex, 21*(6), 1223-1230.

Power, A. J., Reilly, R. B., & Lalor, E. C. (2011). Comparing linear and quadratic models of the human auditory system using EEG. *Conference Proceedings : ...Annual International Conference of the IEEE Engineering in Medicine and Biology Society.IEEE Engineering in Medicine and Biology Society.Conference, 2011*, 4171-4174.

Ravden, D., & Polich, J. (1999). On P300 measurement stability: habituation, intra-trial block variation, and ultradian rhythms. *Biological Psychology, 51*(1), 59-76.

Ream, N. (1970). Nonlinear identification using inverse-repeat m sequences. *Proc.IEE, 117*(1), 213-218.

Regan, D. (1977). Steady-state evoked potentials. *JOSA, 67*(11), 1475-1489.

Reuderink, B. (2008). Games and Brain-Computer Interfaces: The State of the Art. *Enschede: Centre for Telematics and Information Technology University of Twente; Centre for Telematics and Information Technology University of Twente.*

Richardson, T. (2003). Error floors of LDPC codes. Paper presented at the *Proceedings Of The Annual Allerton Conference On Communication Control And Computing, 41*(3) 1426-1435.

Richardson, T. J., Shokrollahi, M. A., & Urbanke, R. L. (2001). Design of capacity-approaching irregular low-density parity-check codes. *Information Theory, IEEE Transactions on, 47*(2), 619-637.

Rothschild, R. M. (2010). Neuroengineering tools/applications for bidirectional interfaces, brain-computer interfaces, and neuroprosthetic implants - a review of recent progress. *Frontiers in Neuroengineering, 3*, 112.

Ryan, W. E. (1998). A turbo code tutorial. Paper presented at the *Proc. IEEE Globecom'98.*

Sarwate, D. V., & Pursley, M. B. (1980). Crosscorrelation properties of pseudorandom and related sequences. *Proceedings of the IEEE, 68*(5), 593-619.

Scherer, R., Schloegl, A., Lee, F., Bischof, H., Jansa, J., & Pfurtscheller, G. (2007). The self-paced graz brain-computer interface: methods and applications. *Computational Intelligence and Neuroscience,* 79826.

Shi, I., & Hecox, K. E. (1991). Nonlinear system identification by m-pulse sequences: Application to brainstem auditory evoked responses. *Biomedical Engineering, IEEE Transactions on, 38*(9), 834-845.

Srebro, R., & Wright, W. W. (1980). Visually Evoked Potentials to Pseudorandom Binary Sequence Stimulation: Preliminary Clinical Trials. *Archives of Ophthalmology, 98*(2), 296-298.

Supin, A. Y. (2008). Discrimination of the spectral structures of sound signals on the background of interference. *Neuroscience and Behavioral Physiology, 38*(5), 477-486.

Supin, A. Y. (2011). Spectrum resolving power of hearing: measurements, baselines, and influence of maskers. *Audiology Research, 1*(2), e27.

Sutter, E. E. (1992). The brain response interface: communication through visually-induced electrical brain responses. *Journal of Microcomputer Applications, 15*(1), 31-45.

Sutter, E. E. (2001). Imaging visual function with the multifocal m-sequence technique. *Vision Research, 41*(10-11), 1241-1255.

Sutter, E. (1985). Multi-input VER and ERG analysis for objective perimetry. Paper presented at the *IEEE/7th Annual Conference of the Engineering in Medicine and Biology Society, 1985,* 415-419.

Swerup, C. (1978). On the choice of noise for the analysis of the peripheral auditory system. *Biological Cybernetics, 29*(2), 97-104.

Tamburrini, G. (2009). *Brain to Computer Communication: Ethical Perspectives on Interaction Models* Springer Netherlands.

Tirkel, A. Z. (1996). Cross correlation of m-sequences-some unusual coincidences. Paper presented at the *Spread Spectrum Techniques and Applications Proceedings, 1996., IEEE 4th International Symposium on, , 3* 969-973 vol. 3.

Toro, C., Deuschl, G., Thatcher, R., Sato, S., Kufta, C., & Hallett, M. (1994). Event-related desynchronization and movement-related cortical potentials on the ECoG and EEG. *Electroencephalography and Clinical Neurophysiology/Evoked Potentials Section, 93*(5), 380-389.

Torrieri, D. (2011). *Principles of spread-spectrum communication systems* Springer Verlag.

Turkmani, A., & Goni, U. (1993). Performance evaluation of maximal-length, Gold and Kasami codes as spreading sequences in CDMA systems. Paper presented at the *Universal Personal Communications, 1993. Personal Communications: Gateway to the 21st Century. Conference Record., 2nd International Conference on, , 2* 970-974 vol. 2.

Velliste, M., Perel, S., Spalding, M. C., Whitford, A. S., & Schwartz, A. B. (2008). Cortical control of a prosthetic arm for self-feeding. *Nature, 453*(7198), 1098-1101.

Vialatte, F. B., Maurice, M., Dauwels, J., & Cichocki, A. (2010). Steady-state visually evoked potentials: focus on essential paradigms and future perspectives. *Progress in Neurobiology, 90*(4), 418-438.

Volosyak, I. (2011). SSVEP-based Bremen–BCI interface—boosting information transfer rates. *Journal of Neural Engineering, 8*, 036020.

Weiskopf, N., Mathiak, K., Bock, S. W., Scharnowski, F., Veit, R., Grodd, W., . . . Birbaumer, N. (2004). Principles of a brain-computer interface (BCI) based on real-time functional magnetic resonance imaging (fMRI). *Biomedical Engineering, IEEE Transactions on, 51*(6), 966-970.

Wolpaw, J. R., Loeb, G. E., Allison, B. Z., Donchin, E., do Nascimento, O. F., Heetderks, W. J., . . . Turner, J. N. (2006). BCI meeting 2005-workshop on signals and recording methods. *Neural Systems and Rehabilitation Engineering, IEEE Transactions on, 14*(2), 138-141.

Wu, D. O. (2012). ***Figure 6.7:*** *Kasami-code generator scheme*. Multimedia Communications and Networking Laboratory (MCN), University of Florida. Retrieved from http://www.wu.ece.ufl.edu/books/EE/communications/CDMA/CDMA.htm on 4/30/2012].

Yekhanin, S. (2006). New locally decodable codes and private information retrieval schemes. Paper presented at the *Electronic Colloquium on Computational Complexity, Vol. TR06,* 127.

Zander, T. O., & Jatzev, S. (2009). Detecting affective covert user states with passive brain-computer interfaces. Paper presented at the *Affective Computing and Intelligent Interaction and Workshops, 2009. ACII 2009. 3rd International Conference on,* 1-9.

Zhang, D., Wang, Y., Maye, A., Engel, A. K., Gao, X., Hong, B., & Gao, S. (2007). A brain-computer interface based on multi-modal attention. Paper presented at the *Neural Engineering, 2007. CNE'07. 3rd International IEEE/EMBS Conference on,* 414-417.

Zhu, D., Bieger, J., Molina, G. G., & Aarts, R. M. (2010). A survey of stimulation methods used in SSVEP-based BCIs. *Computational Intelligence and Neuroscience, 2010*, 1.